

WL-TR-96-2134



VIBRATIONAL ANALYSIS OF A 1/4" STAINLESS STEEL KULITE PROBE

Cameron C. Cunningham, 1Lt, USAF

**Fan and Compressor Branch
Turbine Engine Division**

OCTOBER 1996

FINAL REPORT FOR PERIOD AUGUST 1993 TO JANUARY 1995

Approved for public release; distribution unlimited

DTIC QUALITY INSPECTED 4

**AERO PROPULSION & POWER DIRECTORATE
WRIGHT LABORATORY
AIR FORCE MATERIEL COMMAND
WRIGHT-PATTERSON AIR FORCE BASE, OH 45433-7251**


19970213 030

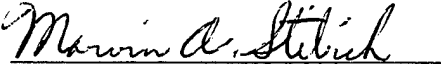
NOTICE

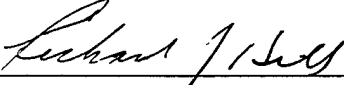
WHEN GOVERNMENT DRAWINGS, SPECIFICATIONS, OR OTHER DATA ARE USED FOR ANY PURPOSE OTHER THAN IN CONNECTION WITH A DEFINITE GOVERNMENT-RELATED PROCUREMENT, THE UNITED STATES GOVERNMENT INCURS NO RESPONSIBILITY OR ANY OBLIGATION WHATSOEVER. THE FACT THAT THE GOVERNMENT MAY HAVE FORMULATED OR IN ANYWAY SUPPLIED THE SAID DRAWINGS, SPECIFICATIONS, OR OTHER DATA, IS NOT TO BE REGARDED BY IMPLICATION, OR OTHERWISE IN ANY MANNER CONSTRUED, AS LICENSING THE HOLDER, OR ANY OTHER PERSON OR CORPORATION; OR AS CONVEYING ANY RIGHTS OR PERMISSION TO MANUFACTURE, USE, OR SELL ANY PATENTED INVENTION THAT MAY IN ANY WAY BE RELATED THERETO.

This report is releasable to the National Technical Information Service (NTIS). At NTIS it will be available to the general public, including foreign nations.

This technical report has been reviewed and is approved for publications.


CAMERON C. CUNNINGHAM, 1Lt, USAF
Fan/Compressor Branch
Turbine Engine Division
Aero Propulsion & Power Directorate


MARVIN A. STIBICH, Chief
Fan/Compressor Branch
Turbine Engine Division
Aero Propulsion & Power Directorate


RICHARD J. HILE
Chief of Technology
Turbine Engine Division
Aero Propulsion & Power Directorate

.If your mailing address has changed, if you wish to be removed from our mailing list, or if the addressee is no longer employed by your organization please notify WL/POTF, Wright-Patterson AFB, OH 45433-6563 to help maintain our current mailing list.

Copies of this report should not be returned unless return is required by security considerations, contractual obligations, or notice on a specific document.

REPORT DOCUMENTATION PAGE			Form Approved OMB No. 0704-0188	
Public reporting burden for this collection of information is estimated to average 1 hour per response, including the time for reviewing instructions, searching existing data sources, gathering and maintaining the data needed, and completing and reviewing the collection of information. Send comments regarding this burden estimate or any other aspect of this collection of information, including suggestions for reducing this burden, to Washington Headquarters Services, Directorate for Information Operations and Reports, 1215 Jefferson Davis Highway, Suite 1204, Arlington, VA 22202-4302, and to the Office of Management and Budget, Paperwork Reduction Project (0704-0188), Washington, DC 20503.				
1. AGENCY USE ONLY (Leave blank)	2. REPORT DATE 1996 October	3. REPORT TYPE AND DATES COVERED Final Report August 1993 to January 1995		
4. TITLE AND SUBTITLE Vibrational Analysis of a 1/4" Stainless Steel Kulite Probe		5. FUNDING NUMBERS PE: 61102 PR: 2307 TA: S1 WU 27		
6. AUTHOR(S) Cameron C. Cunningham, 1Lt, USAF				
7. PERFORMING ORGANIZATION NAME(S) AND ADDRESS(ES) WL/POTF 1950 Fifth St Wright-Patterson AFB, OH 45433-6563		8. PERFORMING ORGANIZATION REPORT NUMBER		
9. SPONSORING/MONITORING AGENCY NAME(S) AND ADDRESS(ES) Turbine Engine Division AeroPropulsion and Power Directorate Air Force Materiel Command Wright-Patterson AFB OH 45433-7251 POC: Cameron C Cunningham, 1Lt; WL/POTF, WPAFB OH 937-255-4738		10. SPONSORING/MONITORING AGENCY REPORT NUMBER WL-TR-96-2134		
11. SUPPLEMENTARY NOTES				
12a. DISTRIBUTION / AVAILABILITY STATEMENT Approved for Public Release; Distribution Unlimited		12b. DISTRIBUTION CODE		
13. ABSTRACT (Maximum 200 words) This report describes the techniques, equipment, and results from the analysis of the frequency response of the 1/4 inch stainless-steel traversing Kulite probe used in the Compressor Aero Research Facility. Through the use of a shake table, the experimental response of the probe was found and compared to a theoretical model.				
14. SUBJECT TERMS Axial Compressor Traverse Probe Gas Turbine			15. NUMBER OF PAGES 50	
			16. PRICE CODE	
17. SECURITY CLASSIFICATION OF REPORT Unclassified	18. SECURITY CLASSIFICATION OF THIS PAGE Unclassified	19. SECURITY CLASSIFICATION OF ABSTRACT Unclassified	20. LIMITATION OF ABSTRACT SAR	

TABLE OF CONTENTS

SECTION	PAGE
List of Illustrations	iii
List of Tables	iv
Nomenclature	v
I INTRODUCTION	1
II BACKGROUND	2
A. Traverse System	3
1. Hardware	4
2. Probes	5
B. Immersion Schedule and Effects	7
III. METHOD	9
A. Theoretical Approach	9
B. Experimental Approach	14
IV. TEST PROCEDURE	22
V RESULTS	24
VI CONCLUSIONS AND RECOMMENDATIONS	33
APPENDIX	35
REFERENCES.....	45

LIST OF ILLUSTRATIONS

FIGURE	PAGE
1. Nylotron Collet	3
2. Rotadata 2-axis Traverse Actuator	4
3. Diagram of the Unsteady Total Pressure Traverse Probe	5
4. Axial and Circumferential Locations of the Traverse Paths	6
5. Forcing Function Diagram	11
6. Schematic of Jig Assembly	16
7. Photograph of the Test Jig	17
8. Photograph of Test Setup	18
9. Schematic of Endevco Accelerometer	19
10. Typical Amplitude Response for Endevco Model 22 Accelerometer	20
11. Photograph of Accelerometer and Probe	20
12. Endevco Model 22 Accelerometer Specifications	21
13. G-Load vs. Immersion Depth @ 6.00 kHz Excitation	27
14. G-Load vs. Immersion Depth @ 6.25 kHz Excitation	28
15. G-Load vs. Immersion Depth @ 6.50 kHz Excitation	29
16. G-Load vs. Immersion Depth @ 6.75 kHz Excitation	30
17. G-Load vs. Immersion Depth @ 7.00 kHz Excitation	31
18. G-Load vs. Immersion Depth @ 7.25 kHz Excitation	32
19. Schematic of Jig Base	42
20. Schematic of Movable Mount	43
21. Schematic of Fixed Mount	44

LIST OF TABLES

TABLE	PAGE
1. Unsteady Total Pressure Probe Specifications	7
2. Probe Immersion Schedule	8
3. Modal Configuration Constants	9
4. Theoretical Natural Frequencies	10
5. Immersion Depth for the First Three Bending Modes	11
6. Probe Force Calculations	12
7. Rotor Speeds and Corresponding Forcing Frequencies	23
8. Load and Immersion of Probe Tip and Collet w.r.t. the Table	35
9. Load and Immersion of Probe Tip and Table w.r.t. the Collet	38

NOMENCLATURE

A	cross-sectional area
C_D	coefficient of drag
D	drag
E	Young's Modulus
F	force
G	acceleration in 'g' units
I	moment of inertia
L	probe length
R	probe radius
V	local velocity
W	force per unit length
d_o	peak displacement
f	frequency
f_n	natural frequency
g	gravity
m	mass density per unit length
q	force distribution
$\beta_n \ell$	configuration constant
ρ	material density
μ	mass per unit length
ω_n	angular frequency

PREFACE

This report was prepared by Cameron C. Cunningham, Second Lieutenant, U.S. Air Force, of the Fan/Compressor Branch, Turbine Engine Division, Aero Propulsion and Power Directorate, Wright Laboratory, Wright-Patterson AFB, Ohio. The work was accomplished between 11 July 1994 and 5 November 1994 and represents results from a portion of the effort of the Compressor Research Group, supervised by Marvin A. Stibich, conducted under Work Unit 27, Task S1, of Project 2307, "Turbomachinery Fluid Dynamic Research." Without the expert technical assistance of Richard Lesley, this work would not have been completed so successfully.

This report describes the techniques, equipment, and results from the analysis of the frequency response of the 1/4 inch stainless-steel traversing Kulite probe used in the Compressor Aero Research Laboratory during the Swept Rotor Study. Through the use of a shake table, the experimental response of the probe was found and compared to a theoretical model. The motivation for this study came from the need to know the validity of Kulite data as it pertains to the traversing system. The final analysis shows that the Kulite probe appears to be severely dampened when subjected to the forcing frequencies of the test rig, probably due to the design of the probe and the traverse system.

SECTION I

INTRODUCTION

This report provides the results of a study on the frequency response of a 1/4 inch stainless-steel probe using both 1) simple cantilever beam analysis for the theoretical search, and 2) simulated test conditions for the experimental venture. The unsteady pressure probe specific to this report was custom-built by Kulite Corporation and is unique to the Compressor Aero Research Laboratory (CARL) facility. As a result, no specific vibrational response data was available on the probe/traverse system.

The theoretical basis for this work lies in simple vibrational analysis. Although conventional formulae cannot be used in this case to provide definitive results, vibrational theory acts as a starting point for performance predictions of the probe/traverse system. This type of modeling will also provide an indication of the areas of interest for the second part of this study - the experimental investigation. The experimental results were given more weight in the final analysis, as this approach provided the decisive results that the theoretical treatise could not.

SECTION II

BACKGROUND

One of the biggest challenges in the experimental research of turbine engine compressors is accurately measuring the unsteady exit conditions of a compressor stage. The forcing function created by the blade-pass frequency is often volatile, especially in high speed experimental research. One measurement device that must perform well under these adverse conditions is the unsteady pressure (Kulite) probe. Although tedious to work with, Kulite probes have shown unsteady total pressures with excellent resolution. By traversing a Kulite probe, a detailed two-dimensional representation of these pressures can be obtained in areas of limited access, such as between a rotor and stator blade-row.

This method of data acquisition, however, is not without its faults. Due to the extreme sensitivity of the Kulite transducer, the accuracy of the readings will diminish if the probe oscillates significantly due to the blade-pass forcing function. This is particularly true at the natural modes of the probe where motion is the greatest. As a result, the vibrational response of the probe must be investigated before any unsteady traverse data can be deemed accurate.

The device used in the Compressor Aero Research Lab is a Kulite high frequency pressure transducer mounted on the tip of a 1/4" stainless steel probe. This probe is placed in a Rotadata actuator, which is mounted on the outside of the compressor test rig

directly behind the rotor. The probe enters the test section through a nylotron bushing which is composed of nylon and graphite and manufactured by Dayton Plastics. This bushing provides an almost air-tight seal, but still allows the probe to slide in and out easily (Figure 1).

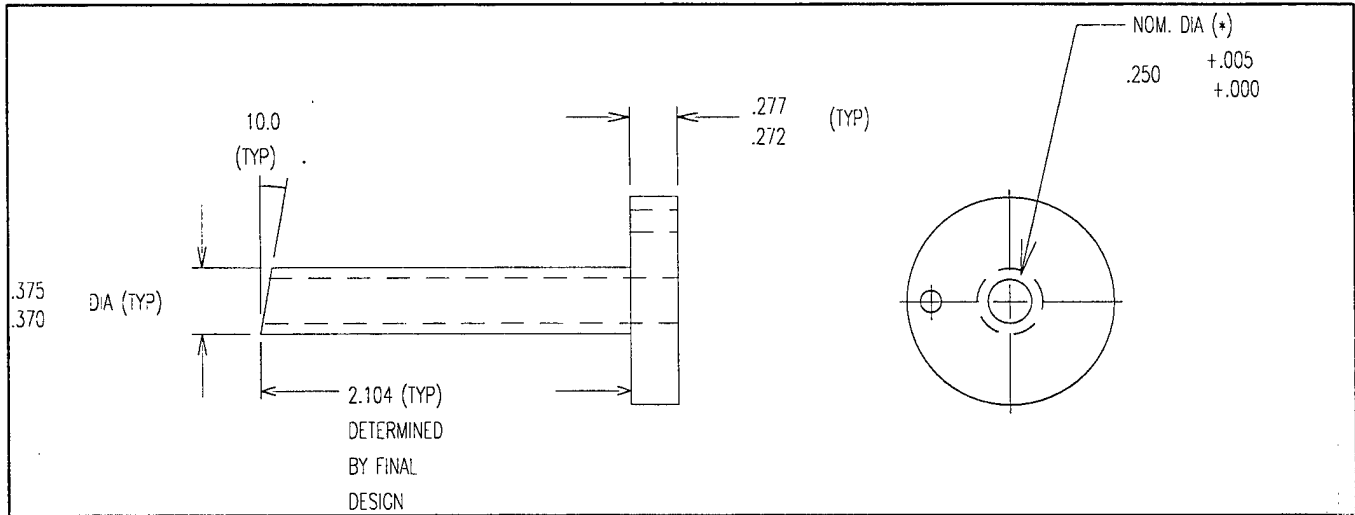


Figure 1. Nylotron Collet

A. Traverse System

A traverse system is employed at CARL to acquire intra-stage (i.e. between the rotor and stator of an axial compressor) traverse data such as temperature, steady and unsteady pressure, and flow angle. The objective of these measurements is two-fold: 1) to directly obtain rotor performance, and 2) to obtain a detailed definition of the rotor exit flowfield, especially in the tip region. Isolating the rotor performance in this way aids future compressor design and can be used to validate CFD codes.

(a) Hardware

The hardware for the traverse system consists of the actuator (with stepper motor), 2-axis controller, various probes, control interface, probe interface and computer interface. A two-axis actuator was mounted on the casing at the exit of rotor. It provides movement in both the radial and yaw (rotation about the direction of radial motion)

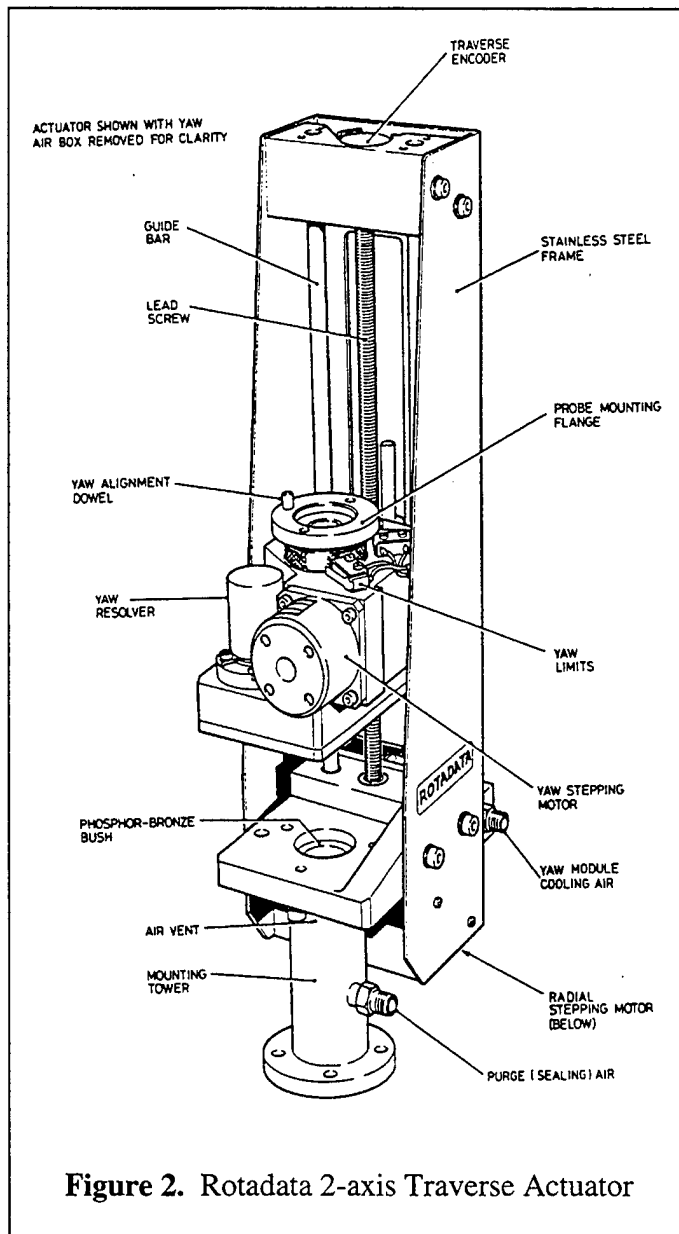


Figure 2. Rotadata 2-axis Traverse Actuator

directions. The actuator and its associated controls were manufactured by Rotadata, Ltd. (Derby, England) and are specifically designed for use in gas turbine engine testing. Figure 2 shows a schematic of the actuator. Mounting locations were provided on the test rig at two different circumferential positions in the same axial plane. The 2-axis C2A controller oversees operations in the radial and angular positions. A control interface converts data from the actuator into a standardized digital format for presentation to

the C2A controller. The probe interface consists of a precision differential pressure transducer with two solenoid calibration valves. Finally, the computer interface allows for external display and control of the system functions.

The actuator moves the Kulite probe inward just aft of the rotor's trailing edge in the spanwise direction. At various immersion distances the probe is stopped, and the Kulite transducer output is recorded simultaneously with a data point that includes typical pressure and temperature data. The total time at any given point is about 60 seconds. Typical rotor speeds (at 100% speed) are around 21,000 rpm, creating relative Mach number as high as 1.4 through a stage.

(b) Probes

The unsteady total pressure probe was a custom designed impact-type probe built by Kulite Corporation. Figure 3 shows the sensing head for this probe. The stem of the probe is made of hollow 1/4" stainless steel tubing which housed the wiring and tubing

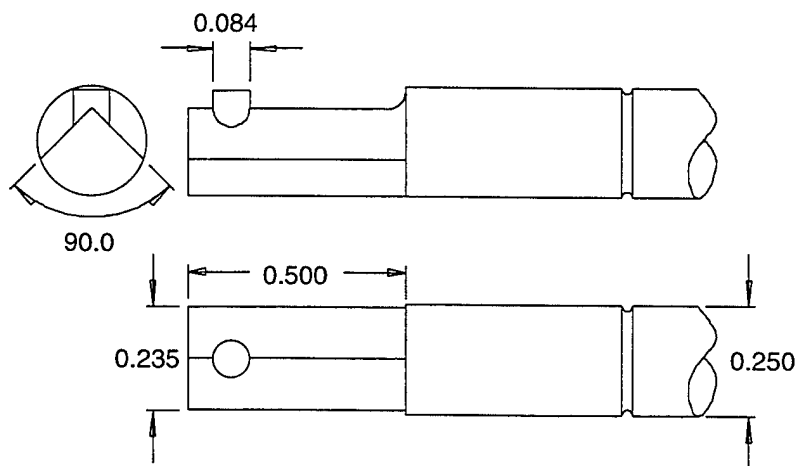


Figure 3. Diagram of the Unsteady Total Pressure Traverse Probe

for the sensing head. The circumferential and axial locations of the traverse paths are given in Figure 4.

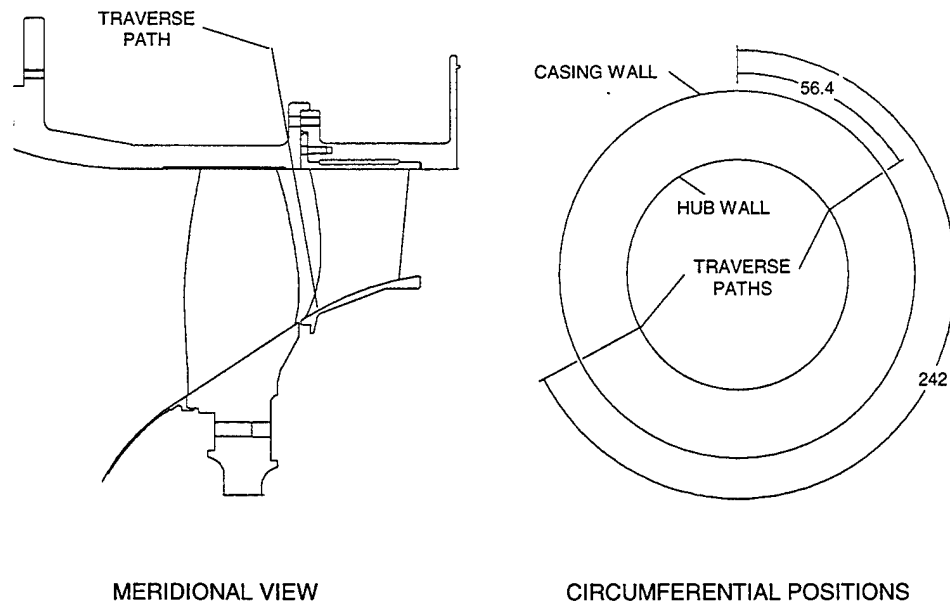


Figure 4. Axial and Circumferential Locations of the Traverse Paths

The probe was held in the actuator by removable pinned collets. The collet clamped around the probe and then fastened to a pinned flange on the actuator. Once the probes were aligned in the radial and yaw directions, the collet was left on the probe for the remainder of the program, allowing for improved repeatability and ease of modification.

A 25-psi differential-type high response transducer was mounted in the probe head with the reference tube extending up the shaft and was open to atmospheric pressure. The casing entrance hole, which was the same diameter as the probe stem (1/4"), limited the size and shape of the probe's head. The supporting electronics were

identical to those described in Cunningham (1996) and are described in Table 1. The unsteady pressure transducer in the probe was calibrated using a Druck model DPI 510 Precision Pressure Controller/Calibrator.

MODEL NO.	SERIAL NO.	RATED PRESSURE (psid)	SENSITIVITY (mV/psid @ 5V DC excitation)	MAXIMUM EXCITATION (Volts DC)
XCQ-118-093-25D	4699-2B-57	25	5.602	7.50

Table 1. Unsteady Total Pressure Probe Specifications

B. Immersion Schedule and Effects

To determine an acceptable immersion schedule, a fine set of data points across the spanwise direction was first recorded. From this, the areas of greatest interest were determined. It was found that the tip region (80-100% span) contained large gradients in all measurements. As a result, the incremental changes were kept small near the outside casing, while a standard 4% change was incorporated for the remainder of the sweep. A typical immersion schedule for SRS is shown in Table 2 with radial distance measured from the centerline of the test rig. The immersion was limited to 20% span and higher due to the relative positioning of the probe and the stator vanes. It was felt that below 20% span the potential field of the stator vanes would invalidate the probe measurements, especially static pressure and measurements derived from static ports (flow angles).

Point No.	Nominal % Span	Radial Position (in.)
1	probes removed	~ 8.9
2	99	8.462
3	98	8.424
4	96	8.346
5	94	8.271
6	92	8.192
7	90	8.115
8	88	8.038
9	84	7.884
10	80	7.729
11	76	7.575
12	72	7.421
13	68	7.267
14	64	7.112
15	60	6.958
16	56	6.804
17	52	6.650
18	48	6.495
19	44	6.341
20	40	6.188
21	36	6.033
22	32	5.878
23	28	5.724
24	24	5.570
25	20	5.416
26	80	7.729
27	probes removed	~ 8.9

Table 2. Probe Immersion Schedule

Throttling effects had to be considered when developing a test plan for traversing. The traverse probes provide a finite amount of local blockage, which is clearly increased the farther the probe is immersed. This can result in a local throttling of the rotor and can be a concern if the presence of the probe changes the rotor's effective operating point. Therefore, this effect was studied carefully in order to determine the best method of operation.

SECTION III

METHOD

A. Theoretical Approach

The classical approach to this problem is to treat the probe as a cantilevered beam. The Kulite would be at the free end, and the point where the probe enters through the nylotron collet would be the fixed end. The beam length will vary with immersion depth, but the fixed end is considered to have zero degrees-of-freedom at any given immersion. The contributions from the torsional modes should be negligible, and thus were ignored in this study. With these assumptions, the natural frequencies can be calculated as follows:

$$f_n = \frac{\omega_n}{2\pi} \quad \text{where} \quad \omega_n = (\beta_n \ell)^2 \left(\frac{EI}{mL^4} \right)^{1/2}$$

The term $\beta_n \ell$ is defined as the configuration constant for a given mode. Table 3 shows these constants.

Mode No.	$\beta_n \ell$
1	1.8751
2	4.6941
3	7.8548

Table 3. Modal Configuration Constants

The probe was determined to be constructed of stainless steel SS 304, which has the properties listed below:

$$E = 28.00 \times 10^6 \text{ psi}$$

$$\mu = 0.00002287 \text{ lb.} \cdot \text{s}^2 / \text{in}^2$$

$$\rho = .286 \text{ lb}_m / \text{in}^3$$

$$I = 0.0001656 \text{ in}^4$$

The moment inertia was found by applying the equation: $I = \frac{\pi}{4}(R_o^4 - R_i^4)$. Use of this

equation is justified because approximately 90% of the probe's immersion length

consisted of a uniform, hollow tube. Only the tip region where the Kulite was housed had

a different cross section, and the cross section for this region was considered tubular for

this study. Table 4 shows the first three angular and natural frequencies of this probe at

various immersion depths.

Mode No.	Probe Length (in.)	ω_n (rad/s)	f_n (Hz)
1	0.5	200,420	31,898
	1.0	50,105	7974
	1.5	22,269	3544
	2.0	12,269	1994
	2.5	8017	1276
	3.0	5567	886
2	0.5	1,256,044	199,906
	1.0	314,011	49,976
	1.5	139,560	22,212
	2.0	78,502	12,494
	2.5	50,242	7996
	3.0	34,890	5553
3	0.5	3,516,869	559,727
	1.0	879,217	139,932
	1.5	390,763	62,192
	2.0	219,804	34,983
	2.5	140,675	22,389
	3.0	97,691	15,548
	3.5	71,773	11,423
	4.0	54,951	8746
	4.5	43,418	6910

Table 4. Theoretical Natural Frequencies

Next, the forcing function on the probe was found. Because the probe is immersed directly aft of the rotor, it sees a once-per-blade perturbation created by the difference in the mass flow rates between the through-passage flow (fairly clean) and the blade wake flow (which possesses a significant velocity deficit).

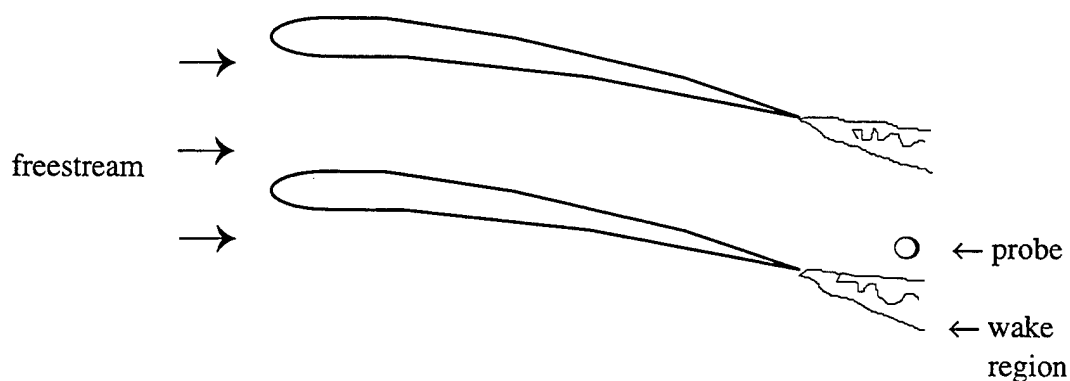


Figure 5. Forcing Function Diagram

In the SRS investigation (Swept Rotor Study) test configuration that accompanied this, the rotor pace at 100% design speed was approximately 21,000 rpm (350 rev/s). The SRS rotors each have 20 blades, so the corresponding forcing frequency is about 7000 Hz. Most measurements in the SRS program were taken at this speed, and as a result, only forcing-frequencies near design speed were investigated. The absolute exit plane Mach number was about 0.75.

Mode No.	Depth (in.) @6.00 kHz	Depth (in.) @6.25 kHz	Depth (in.) @6.50 kHz	Depth (in.) @6.75 kHz	Depth (in.) @7.00 kHz	Depth (in.) @7.25 kHz
1	1.16	1.13	1.11	1.09	1.07	1.05
2	2.90	2.84	2.78	2.73	2.68	2.63
3	4.85	4.75	4.66	4.57	4.49	4.40

Table 5. Immersion Depth for the First Three Bending Modes

Table 5 shows that at 7 kHz, which corresponds to approximately 100% design speed, the probe will cross the first mode just past the one inch immersion, the second mode at just past the 2.6 inches immersion, and the third mode at about 4.5 inches of immersion. Because the SRS test rig could only accommodate a 3.1 inch immersion, modes three and higher could effectively be neglected.

For completeness, the theoretical tip deflection was calculated for full immersion using experimental flow data. The method used here is based on the difference in force that the probe experiences from the passage flow to the wake region. First the drag was calculated using $D = \frac{1}{2} C_D \rho V^2 A$ where $C_D = 1.6$ based on an exit Mach number of 0.75 for a cylinder, and A is the frontal area of the probe at full immersion. From the pressure and temperature measurements from steady-state traverse recording, the local spanwise maxima and minima were calculated for velocity and density. Except near the casing, the spanwise differences in velocity were small, providing a fairly uniform load across the probe. As a result, the average maximum and minimum velocities were found and incorporated into the drag formula. Table 6 shows the results.

	Exit Velocity	Density	Drag
Maxima (averaged)	265.0 m/s	1.58 kg/m ³	4.53 kg (9.98 lb.)
Minima (averaged)	231.6 m/s	1.63 kg/m ³	3.57 kg (7.86 lb.)

Table 6. Probe Force Calculations

From these results, the tip deflection could be estimated, based on the assumption that the probe will deflect fully from the position at maximum force to the position at minimum force. This is a worst-case scenario, as one would not expect a stainless steel tube to be able to complete such a deformation cycle at a speeds in the 7 kHz range.

Local deflection is defined by

$$\delta_{\text{local}} = \frac{-W_a}{24EI} (L - a)^3 (3L + a) - \frac{W_L - W_a}{120EI} (L - a)^3 (4L + a)$$

where 'a' is the distance from the local point of interest to the free end of the probe, and W_L and W_a are the force per unit length at the cantilevered end and the local point interest, respectively. A uniform load was assumed, and only the deflection at the tip ($a=0$) was calculated. The resulting equation is

$$\delta_L = \bar{\delta}_{\text{max}} - \bar{\delta}_{\text{min}} = (\bar{D}_{\text{max}} - \bar{D}_{\text{min}}) \frac{L^3}{8EI}$$

From the above method, the total tip deflection is 0.0000432 meters (0.0017 in). Again, this value represents the total distance the probe tip would move axially due to the one-per-blade force variations and assuming that the probe's response time would be infinitely small; actual deformations should be much smaller. From these assumptions, we would expect the load to on the order of 10^3 Gs, which would most likely destroy the probe - use of the probes have shown that this is not the case.

Also, the possibility exists that the probe may be responding at a frequency which is lower but coincident to the forcing frequency. If this is the case, then theoretical investigations will not prove very fruitful, and an experimental approach must be

adopted. For this reason (and due to the complexity of the probe mounting system and the severity of the theoretical results), an experimental technique was employed to provide a more definitive model of the probe's response.

B. Experimental Approach

The theoretical approach provided a good starting point for the investigation; however, the exact attributes of the traverse system could not be modeled accurately, specifically the interaction between the collet and the probe shaft. The goals of the experimental approach were straightforward - find the first few natural frequencies of the probe at various immersion depths and determine, if possible, the amplitudes of oscillation. This meant that the experiment had to accurately model the characteristics of the Rotadata traverse unit *and* simulate the wake disturbances of the rotor-exit flowfield.

The initial test plan seemed to best meet these goals - attach an accelerometer to the tip of a Kulite probe and run the experiment in the SRS test rig directly. This would have removed most of the variables that would need to be controlled on an 'outside the rig' probe test. However, this approach required total and irreversible destruction of the Kulite probe to run the accelerometer wiring, which was considered unacceptable at that time. In addition, a complete test matrix could not be obtained due to passive excitation.

The next best approach seemed to be a shaker table experiment, which would provide the means to control excitation frequency and amplitude directly. First a jig was designed that would simulate the mounting scheme of the traverse system. A technical

drawing of the jig assembly is shown in Figure 6 and complete engineering drawings of each component are located in the Appendix.

An explanation of the design is in order. First, it must be noted that weight was a driving factor in the design. The shaker table used for the experimental analysis (located in Bld 18g) could not handle more than a few pounds of mass. Excessive weight created distortion when larger amplitudes were applied (for this reason, that actual traverse system could not be tested on the table). On the other hand, the jig had to be fairly sturdy because the jig overlapped the 6" circular mounting surface of the shaker table and could easily introduce a pitchwise bending reaction not found on the actual test hardware. As a result, the jig base was fashioned after a channel beam to provide both maximum pitchwise stability and minimum mass. Aluminum alloy 6061 was chosen for cost, ease of machining, and relative stiffness.

The right side of the jig holds a fixed mount, designed to simulate the test rig wall. The same nylotron collet used on the test was incorporated into the design to simulate its influence on the probe. The left side of the jig held a movable mount, engineered to simulate the motion of the actuator. This mount housed the pinned collet from the Rotadata actuator that clamped on the probe. Also, a slot in the base allowed the mount to slide forward to simulate various immersion depths. Through the use of these mounts, all points of contact with the probe remained unchanged from the original test equipment. Immersion depth would be measured from the tip of the probe to the nylotron collet.

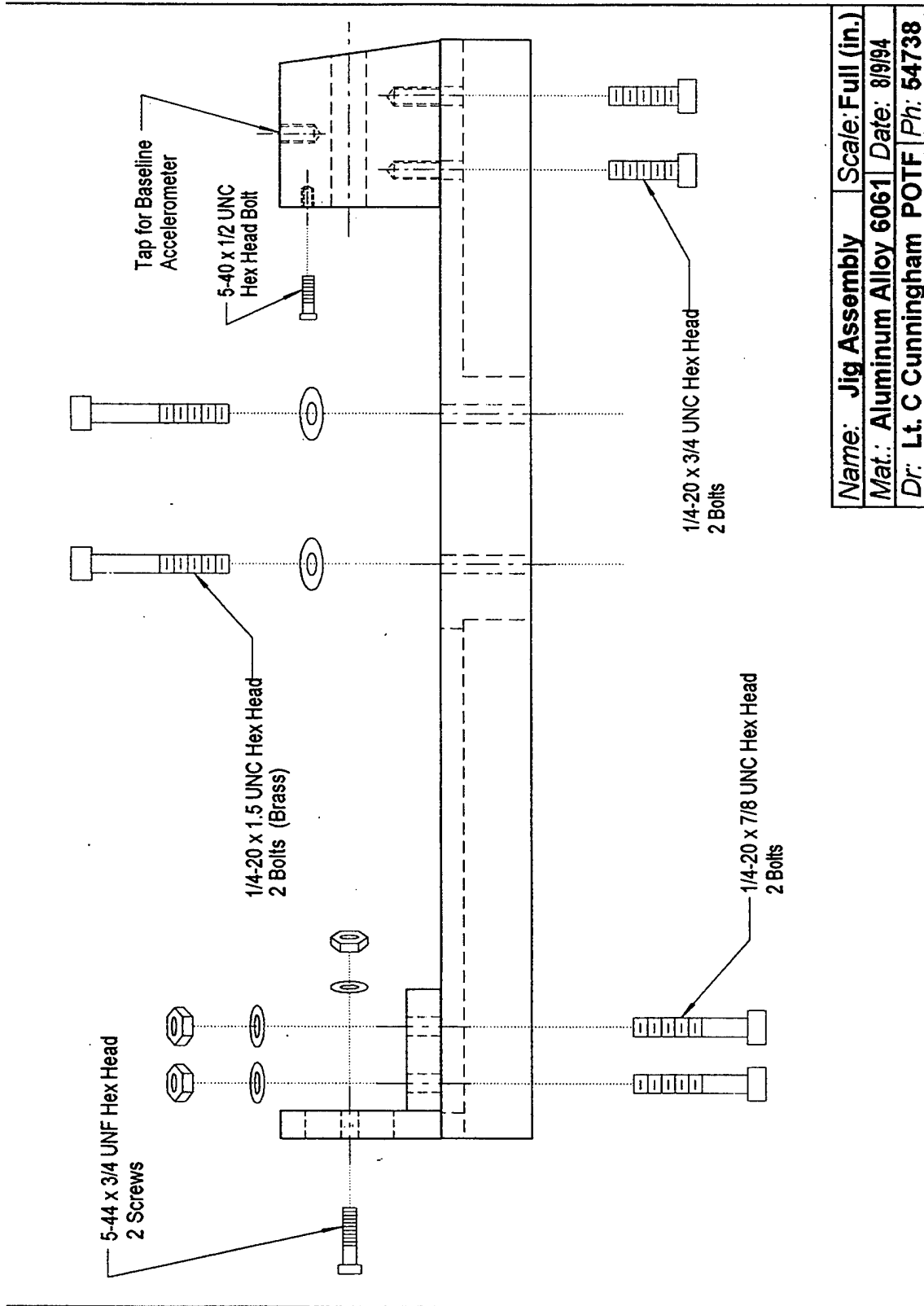


Figure 6. Schematic of Jig Assembly

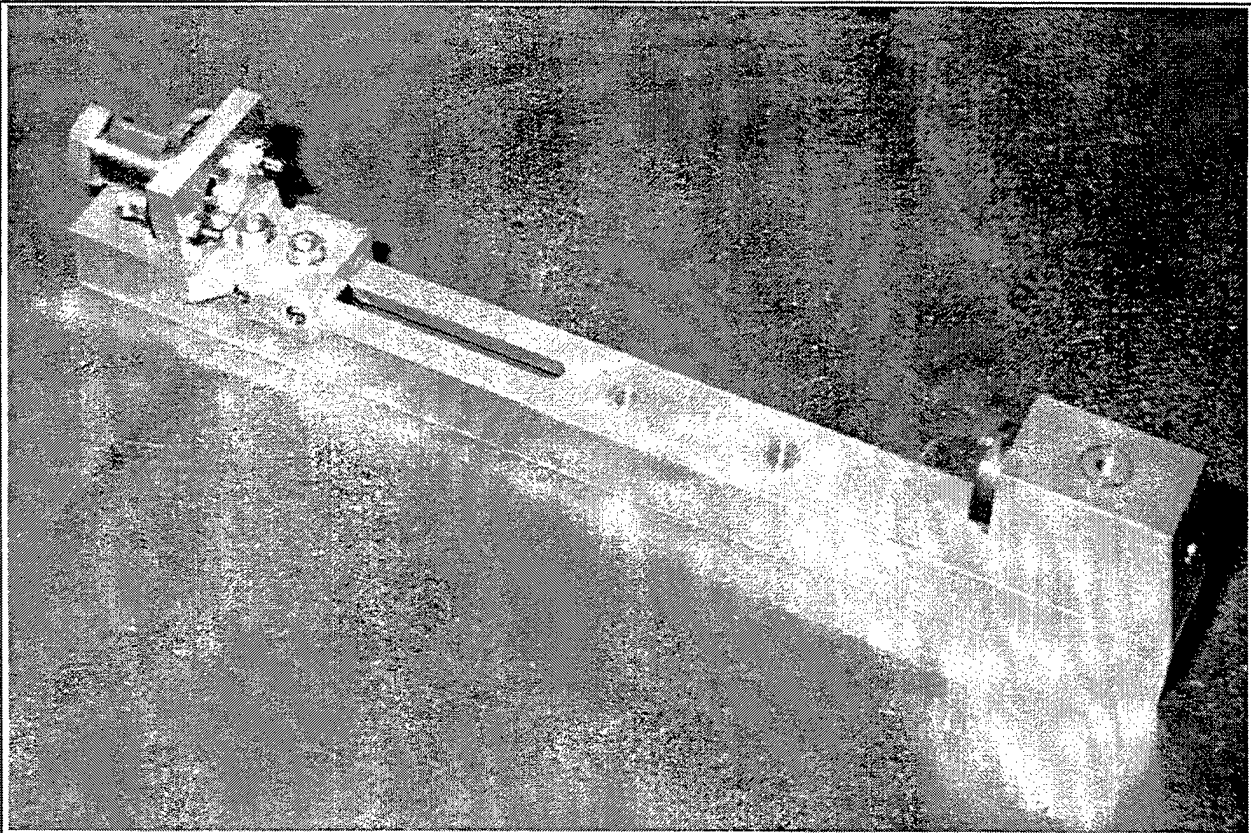


Figure 7. Photograph of Test Jig

To further limit the number of variables, the test would evaluate the response of an unmodified Kulite probe from the SRS program. However, the Kulite sensing surface is extremely sensitive and easily damaged. Therefore, a probe of identical design without the Kulite sensing surface was used for this experiment. This probe still contained the lead wires that ran through the entire length of the inside of the stainless steel tube, which allowed for all the influences of the structure of the probe to remain intact.

The shaker table used in this experiment was the largest one available at WPAFB (Figure 8). The table was excited by a large fabric cone, similar in design to an acoustic



Figure 8. Photograph of Test Setup

speaker. It was capable of vibrating in excess of 100 kHz, with an unloaded amplitude equivalent to 500 Gs. However, with the test jig mounted on the table, the g-load rating was reduced to about 300 @ 7 kHz before distortion appeared. The associated hardware included a charge amplifier containing a controller (for adjusting frequency and amplitude), a signal conditioner, and two oscilloscopes for viewing accelerometer input and/or

output. The controller also housed several needle-type gauges for viewing accelerometer activity.

Three lightweight accelerometers measured the G-loads of the table face, the fixed mount, and the probe tip. The accelerometer on the probe tip needed to be as small (and light) as possible in order to limit its affect on the vibrational responses. The Endevco

Model 22 piezoelectric accelerometer (shown in Figures 9 and 11) seemed well suited for this task for numerous reasons. It weighed only 0.14 grams (one of the lightest in the industry), offered an amplitude response of $\pm 5\%$ deviation from 1 to 10,000 Hz, and provided an amplitude linearity of 1% for loads under 500 Gs. Figure 10 shows the typical amplitude response of this model. Because the Endevco accelerometer was relatively light, its effect on the natural harmonics of the probe was considered negligible. It was adhered to the

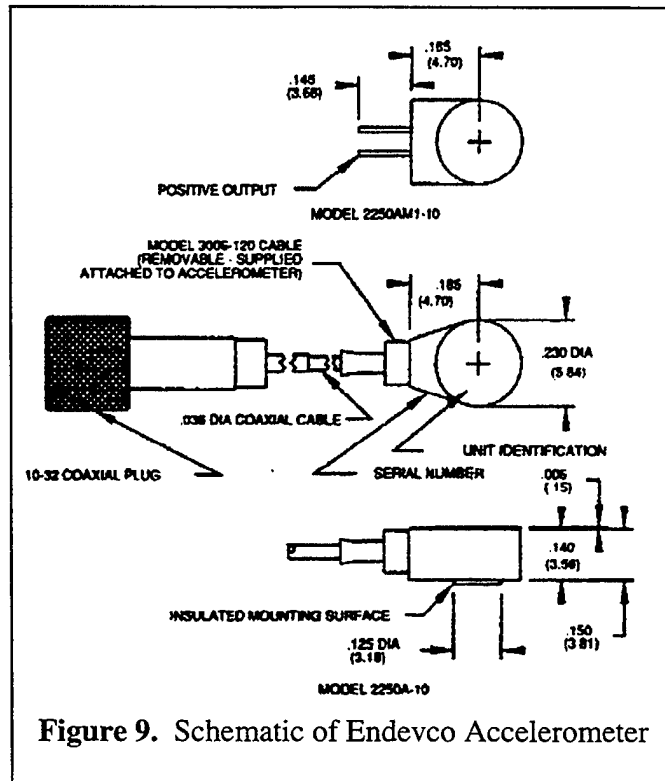
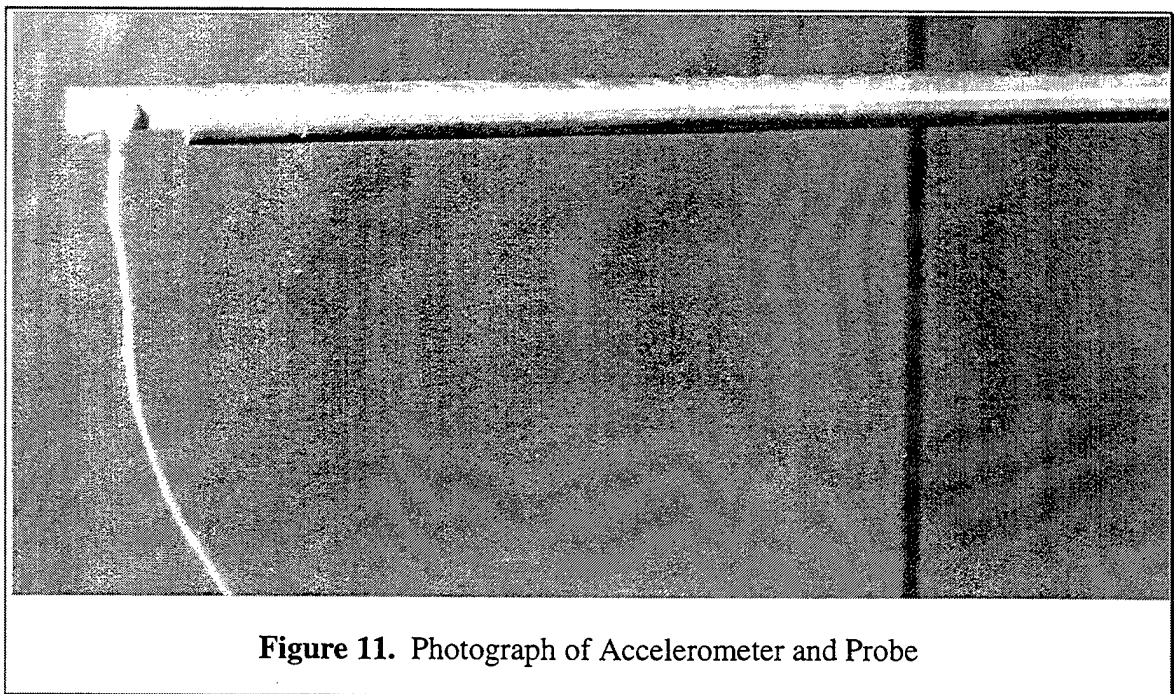
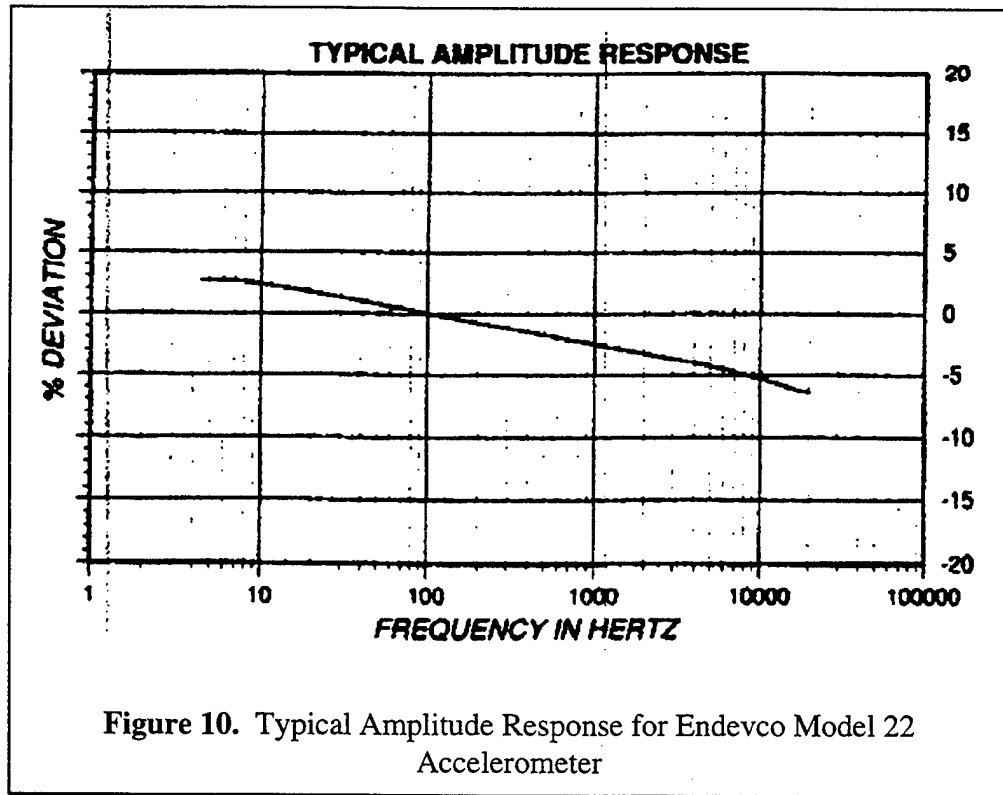


Figure 9. Schematic of Endevco Accelerometer

probe tip on one of the flat surfaces near the Kulite sensing element using cyanoacrylate and was calibrated directly on the shaker table next to a highly accurate baseline accelerometer. The other two accelerometers were calibrated prior to the test and were much larger. These would be screwed one each into the shaker table mounting plate and the fixed mount, providing information on the input loads.

The output from the accelerometers would be accelerations in the form of G-loads. From these, the peak displacements (δ_o) could be found using $\delta_o = 9.780 \cdot G / f^2$ where G is acceleration (in gravitational reference) and f is frequency.



SPECIFICATIONS

The following performance specifications conform to ISA-RP-37.2 (1964) and are typical values, referenced at +75°F (+24°C), 4 mA, and 100 Hz, unless otherwise noted. Calibration data, traceable to National Institute of Standards and Technology (NIST), is supplied.

DYNAMIC CHARACTERISTICS		Units
RANGE	g	± 500
VOLTAGE SENSITIVITY	mV/g	10
± 5%		
FREQUENCY RESPONSE		See Typical Amplitude Response
RESONANCE FREQUENCY	kHz	80
AMPLITUDE RESPONSE		
± 5%	Hz	4 to 2000
± 1dB	Hz	2 to 15 000
TEMPERATURE RESPONSE		See Typical Curve
TRANSVERSE SENSITIVITY	%	≤ 5
AMPLITUDE LINEARITY	%	1 to 500 g
OUTPUT CHARACTERISTICS		
OUTPUT POLARITY		Acceleration directed into base of unit produces positive output.
DC OUTPUT BIAS VOLTAGE	Vdc	+8.5 to +11.5
OUTPUT IMPEDANCE	Ω	≤ 100
RESIDUAL NOISE	equiv. g rms	0.005
2 Hz to 25 kHz, broadband		
GROUNDING		Signal ground connected to case but isolated from mounting surface.
POWER REQUIREMENT		
SUPPLY VOLTAGE	Vdc	+18 to +24
SUPPLY CURRENT	mA	+2 to +20
WARM-UP TIME	sec	< 3
To within 10% of final bias		
ENVIRONMENTAL CHARACTERISTICS		
TEMPERATURE RANGE		-67°F to +257°F (-55°C to +125°C)
HUMIDITY		Epoxy sealed, non-hermetic
SINUSOIDAL VIBRATION LIMIT	g pk	1000
SHOCK LIMIT	g pk	2000
BASE STRAIN SENSITIVITY	equiv. g pk/μ strain	0.0004
THERMAL TRANSIENT SENSITIVITY	equiv. g pk/°F (°C)	0.1 (0.18)
ELECTROMAGNETIC SENSITIVITY	equiv. g rms/gauss	0.0001
PHYSICAL CHARACTERISTICS		
DIMENSIONS		See Outline Drawing
WEIGHT	gm (oz)	0.4 (0.01)
CASE MATERIAL		Anodized aluminum alloy case, beryllium copper lid, alumina mounting surface.
CONNECTOR	2250A-10:	1.2 UNM threads. Recommended connector torque, 0.8 lbf-in (0.09 Nm) or finger tight using wrench.
	2250AM1-10:	Solder terminal, "+" denoted by red dot.
MOUNTING [1]		Flat surface provided for adhesive mounting.
CALIBRATION		
SUPPLIED:		
SENSITIVITY	mV/g	
MAXIMUM TRANSVERSE SENSITIVITY	%	
FREQUENCY RESPONSE	%	20Hz to 10 kHz
	dB	10 kHz to 50 kHz

ACCESSORIES

P/N 22114

ACCELEROMETER REMOVAL TOOL &
CONNECTOR WRENCH FOR 2250A-10
ACCELEROMETER REMOVAL TOOL &
CONNECTOR WRENCH FOR 2250AM1-10
CABLE ASSEMBLY FOR 2250A-10
CABLE ASSEMBLY FOR 2250AM1-10

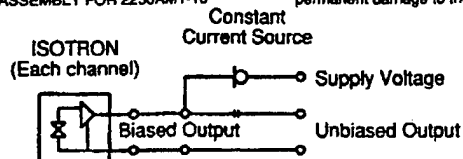
P/N 24385

Model 3006-120 (10 ft)

Model 3024-120 (10 ft)

NOTES

1. Cyanoacrylate adhesives are recommended for temporary mounting applications. To remove the accelerometer, soften the adhesive with the appropriate solvent and use the removal tool supplied with each accelerometer. Striking or applying excessive torque to break the glue bond will cause permanent damage to the transducer.



Continued product improvement necessitates that Endevco reserve the right to modify these specifications without notice. Endevco maintains a program of constant surveillance over all products to ensure a high level of reliability. This program includes attention to reliability factors during product design, the support of stringent Quality Control requirements, and compulsory corrective action procedures. These measures, together with conservative specifications have made the name Endevco synonymous with reliability.

TOTAL P. 03

Figure 12. Endevco Model 22 Accelerometer Specifications

SECTION IV

TEST PROCEDURE

The goal of the shaker table test was to find the first two or three natural frequencies of the probe and the amplitudes of oscillation at various immersion depths and input frequencies. The original test plan called for a 3 x 6 test matrix:

- Input frequencies of 6.0, 6.5, and 7.0 kHz
- Six immersion depths varying from 1.0 to 4.0 inches

Once the natural frequencies were found, various G-loads would be applied at that mode to determine the amplitude of response of the probe head. This test plan was altered as discussed below.

The jig/probe system was bolted to the shaker table. The three accelerometers were calibrated beforehand and their output could be monitored simultaneously (in Gs) - one each on the table face, top of the fixed mount, and on the probe head. With the weight of the jig, the table was originally expected to deliver less than 10 Gs before distortion occurred. The first test was to determine the maximum G-load that the table could cleanly input. In the frequency range of interest (6.0-7.25 kHz), it was soon discovered that the table could excite at over 100 Gs, as read by the table mounted accelerometer. This value (100 Gs) was subsequently used for the input load, as it seemed to depict more accurately the real test conditions at CARL.

The controller had simple dials that allowed quick changes to the frequency and amplitude inputs. Consequently, the test plan was expanded to include 6.0, 6.25, 6.5, 6.75, 7.0, and 7.25 kHz, and immersion depths varying from 1.000 to 4.000 inches by increments of 0.125" to provide a more comprehensive simulation of test conditions (see Table 7). Also, initial observations showed that the input load to the table did not always match the input load on the fixed mount. If the jig was perfectly rigid, these inputs would have been identical at all times. It was difficult to determine which had a greater influence on the probes' response - the table or the nylotron collet. Therefore, both the table and the fixed mount were given the control load (100 Gs) for the entire data set. The final test matrix was 6 x 25 x 2.

Rotor Speed (RPM)	Percentage of Design Speed	Corresponding Forcing Freq. (Hz)
18,000	85%	6000
18,750	90%	6250
19,500	93%	6500
20,250	96%	6750
21,000	100%	7000
21,750	104%	7250

Table 7. Rotor Speeds and Corresponding Forcing Frequencies

SECTION IV

RESULTS

Figures 13 through 18 show the acceleration vs. immersion depth at each of the six frequencies and for each control condition. These results show that the shaker table and the fixed mount with the nylotron collet do not always experience the same input amplitude - obviously the jig was not as rigid as originally thought. This was probably due to the design assumption of a maximum 10g load, not 100g. Displacements were also calculated, but are not graphed here; because the frequency remains constant on these graphs, the displacement plots are characteristically identical.

Overall, the probe did not seem to show any tendencies toward large oscillations, even when the control load was switched. Also, several impromptu experiments were done in an attempt to radically excite the probe head; various frequencies, loads, and immersion depths were applied, but no modal responses were ever found. Furthermore, only one condition in the test matrix (Figure 15) excited the probe head above the 100g input. Even at this point, the response was only 105 Gs. In general, the probe tip's actions *qualitatively* mimicked that of the table surface.

A closer inspection of Figures 13 through 18 is required. At 6.00 kHz, the probe responded at 30% or less of the 100g input for both control loads. The lower plot shows that the probe's amplitude tended to follow that of the table surface, not the nylotron

mount. The top plot supports this. Even when the nylotron mount responded at 350 Gs, the probe was not significantly influenced. Overall, the probe showed little excitation at this frequency. Similar results were found at 6.25 kHz, with one minor difference. The amplitude output was slightly higher across at all immersions, and particularly from 2.25 to 3.50 inch immersion.

At 6.50 and 6.75 kHz, comparable results were found. Each shows that the nylotron mount became highly excited (top graphs), indicating that the collet and/or jig must have a natural frequency in this area. Although the probe responded more at these points, the relatively massive motion of the collet may taint any attempt at interpretation. The lower graphs, where the bushing amplitude was fixed, show how closely the probe tip's and the table's amplitudes compare.

The last two frequencies, 7.00 and 7.25 kHz, show a different trend entirely. At these frequencies the probe tip appears highly damped, rarely reaching even 20% of the input value (for either control load).

Collectively, these results seem to indicate that the current mounting scheme tends to dampen the probe. Even though the probe responded the most at 6.50 kHz and to a lesser extent 6.75 kHz, the magnitudes were never significantly more than the input load. One would expect a response higher than the excitation amplitude at the natural frequency of the probe were it not damped. Also, the 'impromptu' experiments (which included exciting the table to the point of distortion and immersing the probe to the

predicted mode depths) indicated a genuine lack of response. There seems to be no correlation between the predicted natural frequencies and the occasional rises in probe amplitude. What little response the probe offers appears to be driven only by the composition of the mounting system.

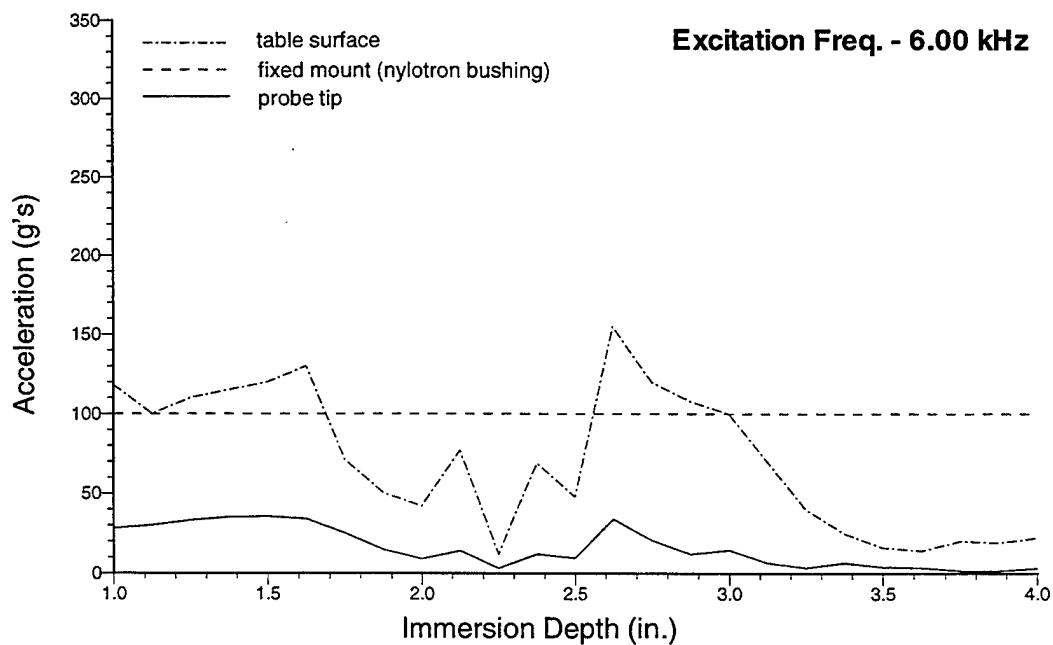
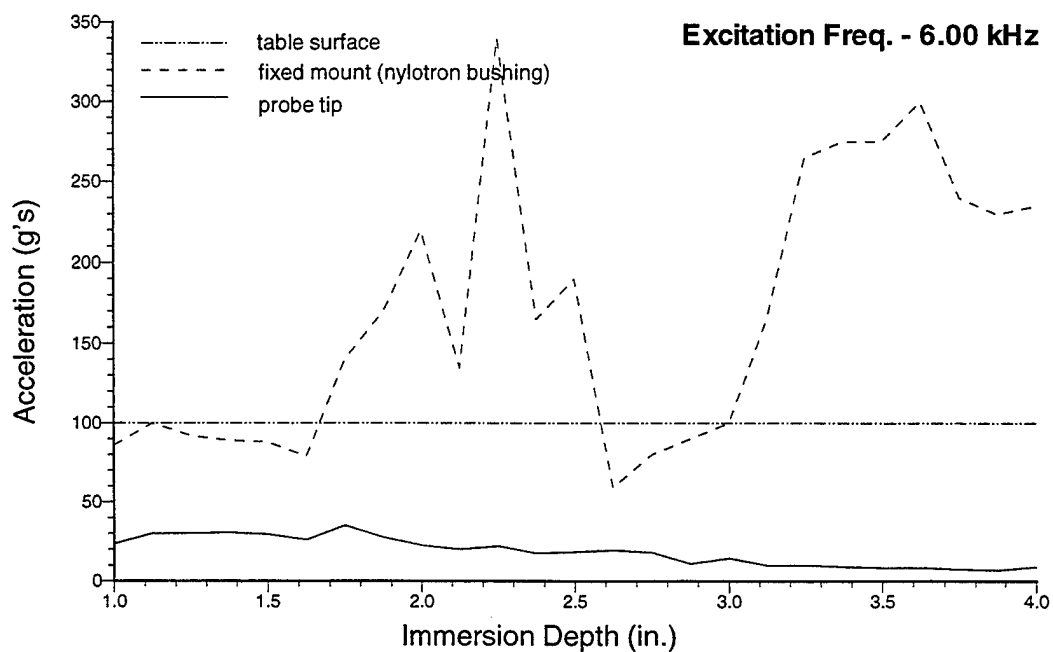


Figure 13. G-Load vs. Immersion Depth @ 6.00 kHz Excitation

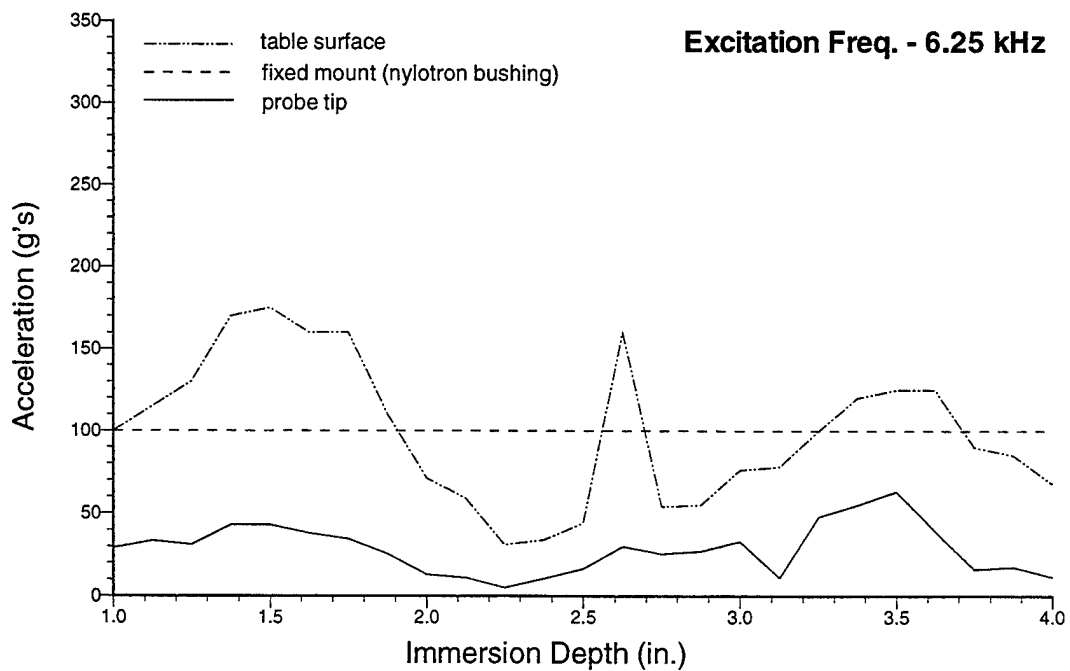
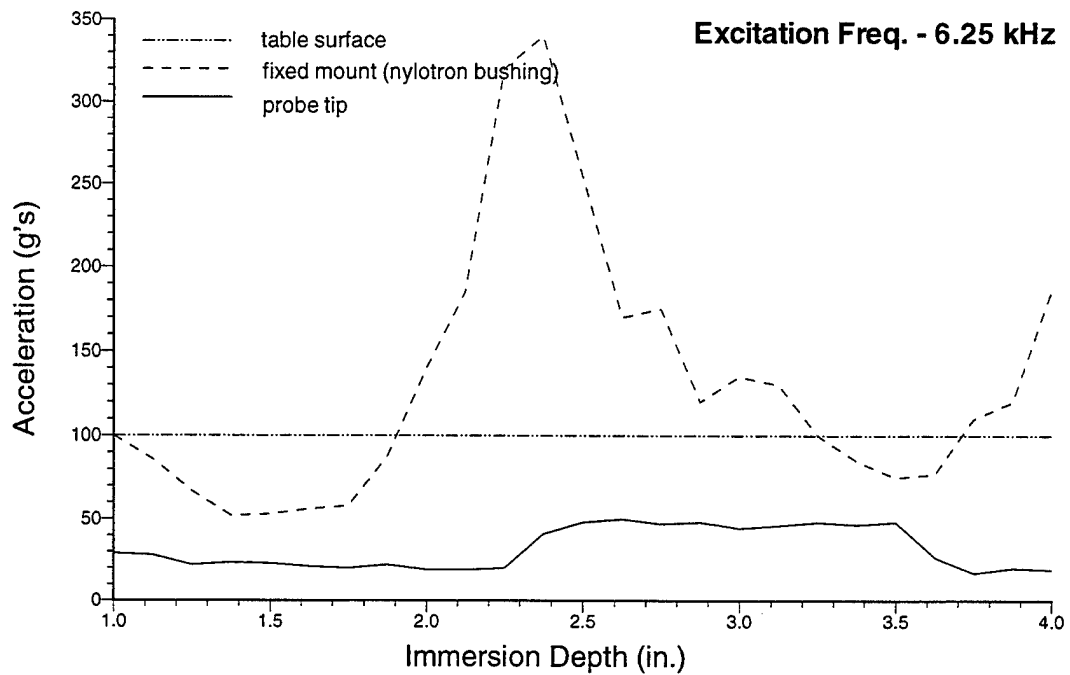


Figure 14. G-Load vs. Immersion Depth @ 6.25 kHz Excitation

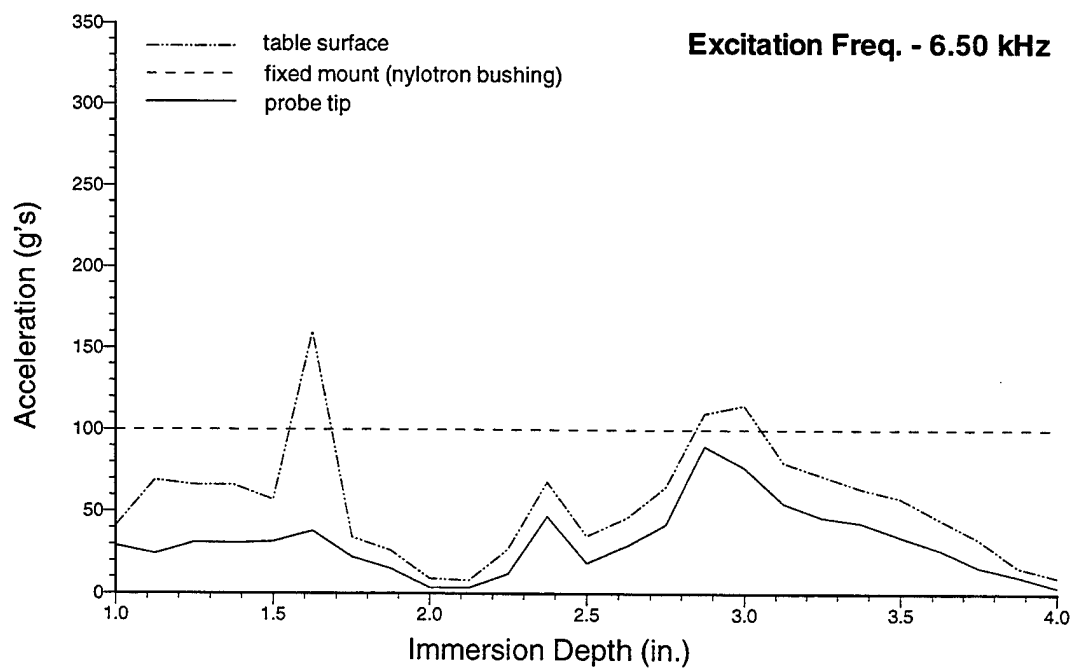
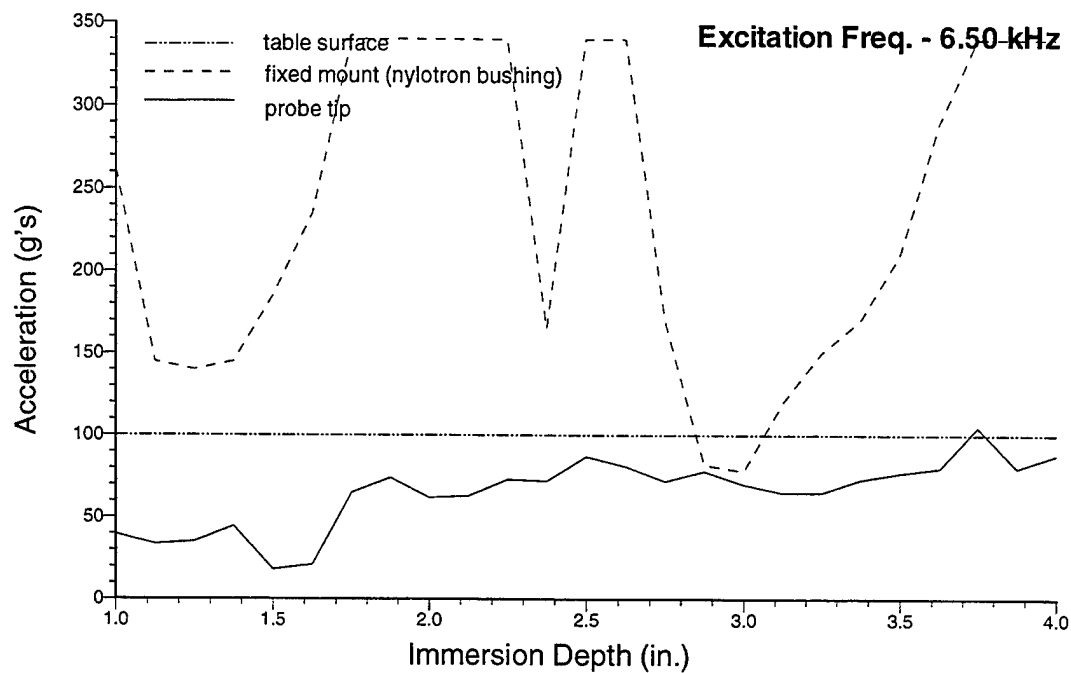


Figure 15. G-Load vs. Immersion Depth @ 6.50 kHz Excitation

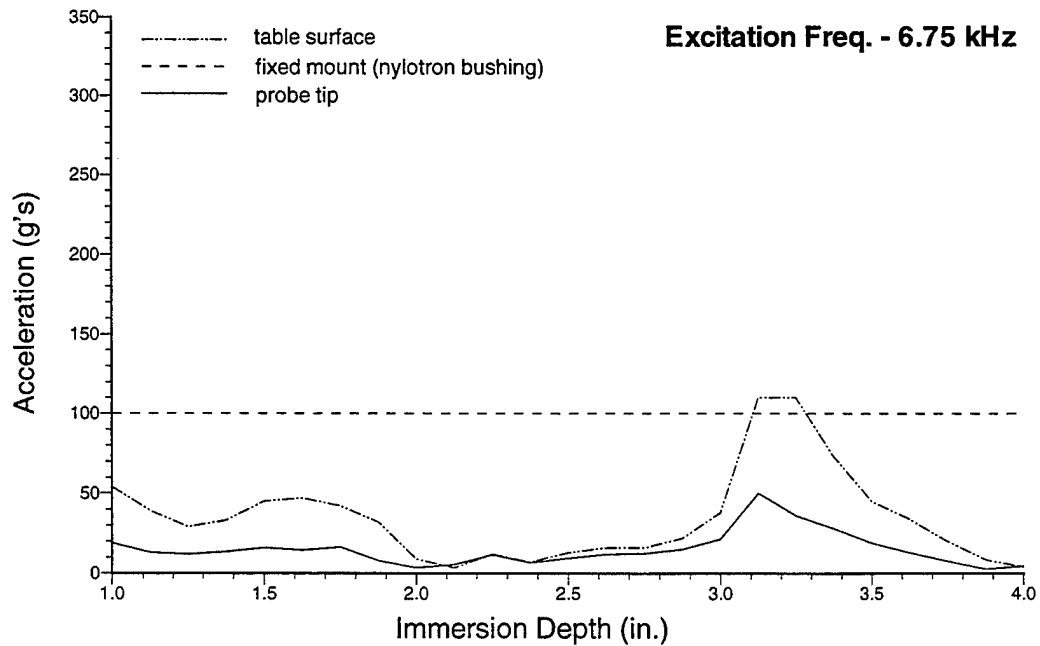
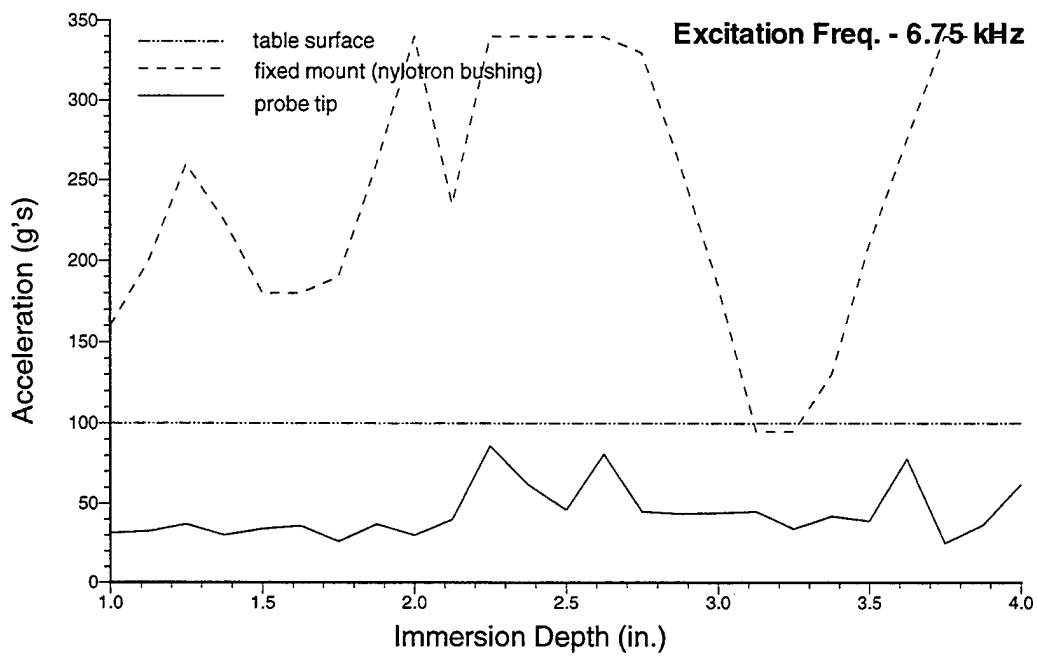


Figure 16. G-Load vs. Immersion Depth @ 6.75 kHz Excitation

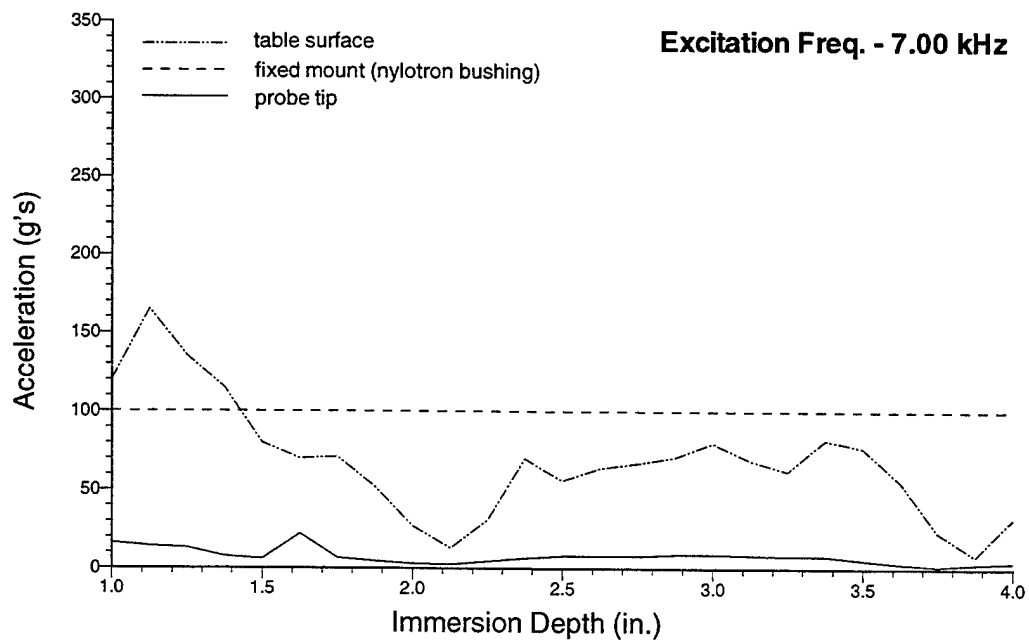
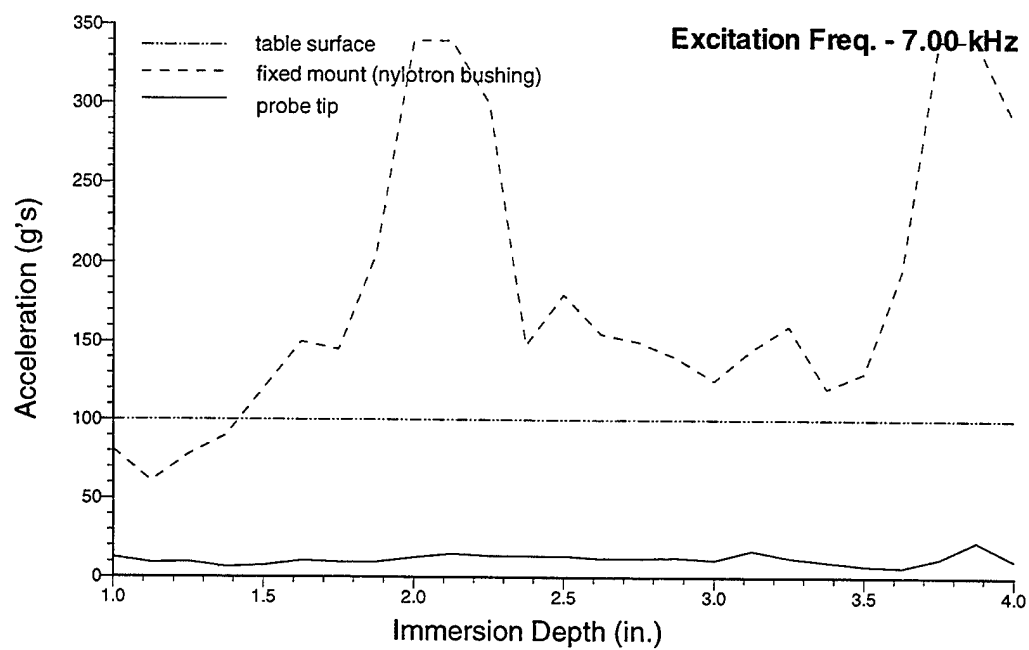


Figure 17. G-Load vs. Immersion Depth @ 7.00 kHz Excitation

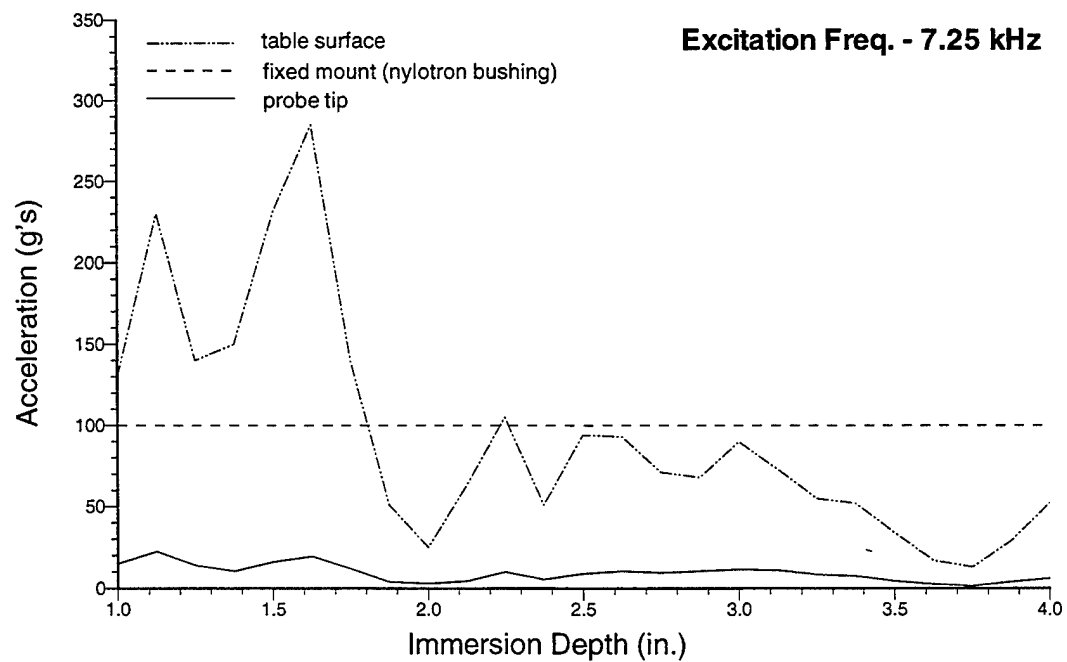
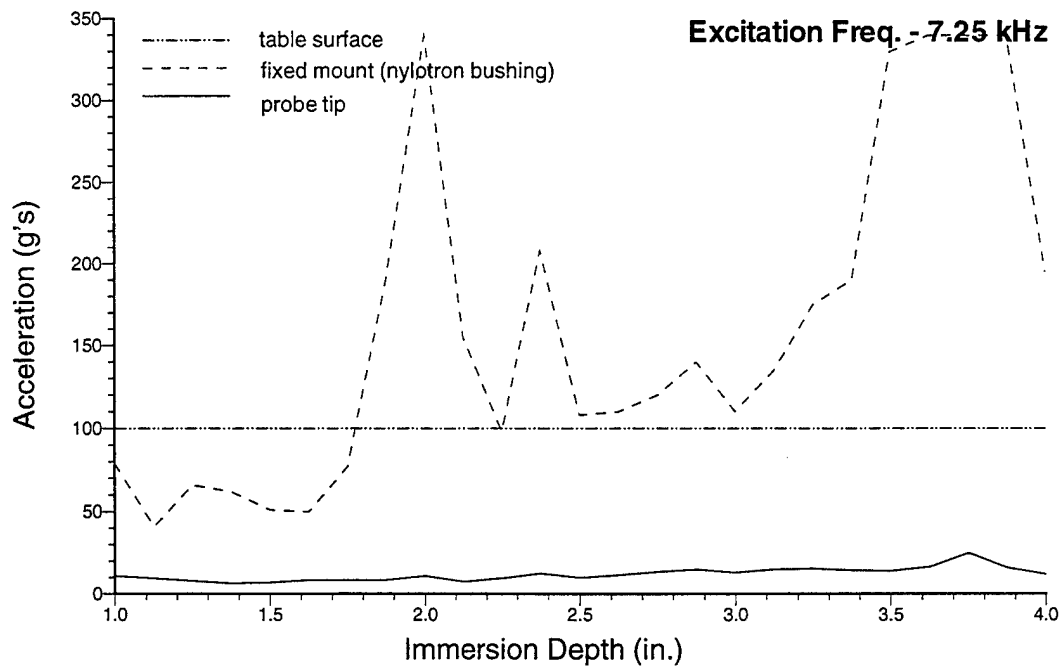


Figure 18. G-Load vs. Immersion Depth @ 7.25 kHz Excitation

SECTION V

CONCLUSIONS & RECOMMENDATIONS

The results from this study seem to indicate that the traversed Kulite probe will not become modally excited when used in the traverse configuration from the Swept Rotor Study, even at the predicted modal points. Although both the test jig and the shaker table had evident natural modes, the probe tip could not be significantly excited at or near any of its predicted natural frequencies. The probe seems to have been vibrationally dampened by the mounting system in which it was held.

Several reasons could attribute to the lack of response from the probe's tip, including damping from the nylotron collet and internal wiring, the lack of a fixed cantilever point, probe geometry, and experimental errors. Damping seems to be the most likely explanation. The internal wiring and especially the collet, which has some plastic characteristic, create a non-rigid environment that may absorb much of the kinetic energy released from the probe during excitation. The internal wiring occupies the entire void within the probe's shaft, thus changing the effective Modulus of Elasticity of the probe. A simple test shows that the probe (alone) will not resonate at any audible frequency when struck with a mallet. Although not conclusive, this suggests that the internal wiring and epoxy may limit the excitation of the probe. The nylotron collet appears to be the major damping source, providing not only a relatively flexible surface around the probe shaft, but also a finite, radial tolerance. The resulting multidimensional

slippage created a fairly loose cantilever point that may absorb vibrational energy better than translating it. The theoretical model seems invalid because it assumes a firm, fixed point at the end of the collet. The experimental data shows that the aluminum mount holding the collet was usually excited to higher degree than the probe tip, supporting the energy-absorption argument. If the collet was able to transfer more of the vibrational energy, one would expect the probe tip and the collet mount to respond similarly.

The data also supports the notion that the fixed point on the probe has more influence on tip response than the nylotron collet. During actual testing at CARL where airflow drives the probe's motion, the clamped end does not vibrate because it is located outside the test rig. Thus, the fixed end will help dampen the probe. In addition, the nylotron collet absorbs most of the energy from the forcing function.

In conclusion, this test indicates that the unsteady pressure data from SRS should be unaffected by the blade-pass forcing function of the rotor. The probe did not show any natural modes in this experiment, but appeared to be highly dampened. Varying the immersion depth did produce a dramatic change in probe response. Output amplitudes typically fell well below the input values, particularly at blade-pass frequencies corresponding to 21,000 rpm (~ 100% speed) where the response was almost zero.

In the future, every effort should be made to perform this experiment in the actual test configuration during a test run. This will remove all the variables from the shaker table and jig, and the probe will be excited at with the proper load and load distribution.

APPENDIX

Excitation Frequency (Hz)	Probe Immersion (inches)	Table Acceleration (Gs)	Table Displacement (inches)	Nylotron Collet Acceleration	Nylotron Collet Displacement	Probe Tip Acceleration (Gs)	Probe Tip Displacement (inches)
6000	1.000	100.0	0.0000272	86.0	0.0000234	23.5	0.0000064
6000	1.125	100.0	0.0000272	100.0	0.0000272	30.0	0.0000082
6000	1.250	100.0	0.0000272	92.0	0.0000250	30.0	0.0000082
6000	1.375	100.0	0.0000272	89.0	0.0000242	30.5	0.0000083
6000	1.500	100.0	0.0000272	88.0	0.0000239	29.5	0.0000080
6000	1.625	100.0	0.0000272	79.0	0.0000215	26.0	0.0000071
6000	1.750	100.0	0.0000272	140.0	0.0000380	35.0	0.0000095
6000	1.875	100.0	0.0000272	170.0	0.0000462	27.5	0.0000075
6000	2.000	100.0	0.0000272	220.0	0.0000598	22.5	0.0000061
6000	2.125	100.0	0.0000272	135.0	0.0000367	20.0	0.0000054
6000	2.250	100.0	0.0000272	340.0	0.0000924	22.0	0.0000060
6000	2.375	100.0	0.0000272	165.0	0.0000448	17.5	0.0000048
6000	2.500	100.0	0.0000272	190.0	0.0000516	18.5	0.0000050
6000	2.625	100.0	0.0000272	59.0	0.0000160	19.5	0.0000053
6000	2.750	100.0	0.0000272	80.0	0.0000217	18.0	0.0000049
6000	2.875	100.0	0.0000272	90.0	0.0000244	11.0	0.0000030
6000	3.000	100.0	0.0000272	100.0	0.0000272	14.5	0.0000039
6000	3.125	100.0	0.0000272	165.0	0.0000448	10.0	0.0000027
6000	3.250	100.0	0.0000272	265.0	0.0000720	10.0	0.0000027
6000	3.375	100.0	0.0000272	275.0	0.0000747	9.0	0.0000024
6000	3.500	100.0	0.0000272	275.0	0.0000747	8.5	0.0000023
6000	3.625	100.0	0.0000272	300.0	0.0000815	8.5	0.0000023
6000	3.750	100.0	0.0000272	240.0	0.0000652	7.5	0.0000020
6000	3.875	100.0	0.0000272	230.0	0.0000625	7.0	0.0000019
6000	4.000	100.0	0.0000272	235.0	0.0000638	9.0	0.0000024
6250	1.000	100.0	0.0000250	100.0	0.0000250	29.0	0.0000073
6250	1.125	100.0	0.0000250	86.0	0.0000215	28.0	0.0000070
6250	1.250	100.0	0.0000250	67.0	0.0000168	22.0	0.0000055
6250	1.375	100.0	0.0000250	52.0	0.0000130	23.5	0.0000059
6250	1.500	100.0	0.0000250	53.0	0.0000133	23.0	0.0000058
6250	1.625	100.0	0.0000250	56.0	0.0000140	21.0	0.0000053
6250	1.750	100.0	0.0000250	58.0	0.0000145	20.0	0.0000050
6250	1.875	100.0	0.0000250	88.0	0.0000220	22.0	0.0000055
6250	2.000	100.0	0.0000250	140.0	0.0000351	19.0	0.0000048
6250	2.125	100.0	0.0000250	185.0	0.0000463	19.0	0.0000048
6250	2.250	100.0	0.0000250	320.0	0.0000801	20.0	0.0000050
6250	2.375	100.0	0.0000250	340.0	0.0000851	41.0	0.0000103
6250	2.500	100.0	0.0000250	255.0	0.0000638	48.0	0.0000120
6250	2.625	100.0	0.0000250	170.0	0.0000426	50.0	0.0000125
6250	2.750	100.0	0.0000250	175.0	0.0000438	47.0	0.0000118
6250	2.875	100.0	0.0000250	120.0	0.0000300	48.0	0.0000120

Table 8. Load and Immersion of Probe Tip and Collet w.r.t. the Table

Excitation Frequency (Hz)	Probe Immersion (inches)	Table Acceleration (Gs)	Table Displacement (inches)	Nylotron Collet Acceleration	Nylotron Collet Displacement	Probe Tip Acceleration (Gs)	Probe Tip Displacement (inches)
6250	3.000	100.0	0.0000250	135.0	0.0000338	44.5	0.0000111
6250	3.125	100.0	0.0000250	130.0	0.0000325	46.0	0.0000115
6250	3.250	100.0	0.0000250	100.0	0.0000250	48.0	0.0000120
6250	3.375	100.0	0.0000250	85.0	0.0000213	46.5	0.0000116
6250	3.500	100.0	0.0000250	75.0	0.0000188	48.0	0.0000120
6250	3.625	100.0	0.0000250	77.0	0.0000193	26.5	0.0000066
6250	3.750	100.0	0.0000250	110.0	0.0000275	17.0	0.0000043
6250	3.875	100.0	0.0000250	120.0	0.0000300	20.0	0.0000050
6250	4.000	100.0	0.0000250	185.0	0.0000463	19.0	0.0000048
6500	1.000	100.0	0.0000231	262.0	0.0000606	39.5	0.0000091
6500	1.125	100.0	0.0000231	145.0	0.0000336	33.5	0.0000078
6500	1.250	100.0	0.0000231	140.0	0.0000324	35.0	0.0000081
6500	1.375	100.0	0.0000231	145.0	0.0000336	44.5	0.0000103
6500	1.500	100.0	0.0000231	185.0	0.0000428	18.0	0.0000042
6500	1.625	100.0	0.0000231	235.0	0.0000544	21.0	0.0000049
6500	1.750	100.0	0.0000231	340.0	0.0000787	65.0	0.0000150
6500	1.875	100.0	0.0000231	340.0	0.0000787	74.0	0.0000171
6500	2.000	100.0	0.0000231	340.0	0.0000787	62.0	0.0000144
6500	2.125	100.0	0.0000231	340.0	0.0000787	63.0	0.0000146
6500	2.250	100.0	0.0000231	340.0	0.0000787	73.0	0.0000169
6500	2.375	100.0	0.0000231	165.0	0.0000382	72.0	0.0000167
6500	2.500	100.0	0.0000231	340.0	0.0000787	87.0	0.0000201
6500	2.625	100.0	0.0000231	340.0	0.0000787	81.0	0.0000187
6500	2.750	100.0	0.0000231	170.0	0.0000394	72.0	0.0000167
6500	2.875	100.0	0.0000231	82.0	0.0000190	78.0	0.0000181
6500	3.000	100.0	0.0000231	78.0	0.0000181	70.0	0.0000162
6500	3.125	100.0	0.0000231	120.0	0.0000278	65.0	0.0000150
6500	3.250	100.0	0.0000231	150.0	0.0000347	65.0	0.0000150
6500	3.375	100.0	0.0000231	170.0	0.0000394	73.0	0.0000169
6500	3.500	100.0	0.0000231	210.0	0.0000486	77.0	0.0000178
6500	3.625	100.0	0.0000231	290.0	0.0000671	80.0	0.0000185
6500	3.750	100.0	0.0000231	340.0	0.0000787	105.0	0.0000243
6500	3.875	100.0	0.0000231	340.0	0.0000787	80.0	0.0000185
6500	4.000	100.0	0.0000231	340.0	0.0000787	88.0	0.0000204
6750	1.000	100.0	0.0000215	160.0	0.0000343	31.5	0.0000068
6750	1.125	100.0	0.0000215	200.0	0.0000429	32.5	0.0000070
6750	1.250	100.0	0.0000215	260.0	0.0000558	37.0	0.0000079
6750	1.375	100.0	0.0000215	225.0	0.0000483	30.0	0.0000064
6750	1.500	100.0	0.0000215	180.0	0.0000386	34.0	0.0000073
6750	1.625	100.0	0.0000215	180.0	0.0000386	36.0	0.0000077
6750	1.750	100.0	0.0000215	190.0	0.0000408	26.0	0.0000056
6750	1.875	100.0	0.0000215	260.0	0.0000558	37.0	0.0000079
6750	2.000	100.0	0.0000215	340.0	0.0000730	30.0	0.0000064
6750	2.125	100.0	0.0000215	235.0	0.0000504	40.0	0.0000086
6750	2.250	100.0	0.0000215	340.0	0.0000730	86.0	0.0000185

Table 8. Load and Immersion of Probe Tip and Collet w.r.t. the Table (cont.)

Excitation Frequency (Hz)	Probe Immersion (inches)	Table Acceleration (Gs)	Table Displacement (inches)	Nylotron Collet Acceleration	Nylotron Collet Displacement	Probe Tip Acceleration (Gs)	Probe Tip Displacement (inches)
6750	2.375	100.0	0.0000215	340.0	0.0000730	62.0	0.0000133
6750	2.500	100.0	0.0000215	340.0	0.0000730	46.0	0.0000099
6750	2.625	100.0	0.0000215	340.0	0.0000730	81.0	0.0000174
6750	2.750	100.0	0.0000215	330.0	0.0000708	45.0	0.0000097
6750	2.875	100.0	0.0000215	260.0	0.0000558	43.5	0.0000093
6750	3.000	100.0	0.0000215	185.0	0.0000397	44.0	0.0000094
6750	3.125	100.0	0.0000215	95.0	0.0000204	45.0	0.0000097
6750	3.250	100.0	0.0000215	95.0	0.0000204	34.0	0.0000073
6750	3.375	100.0	0.0000215	130.0	0.0000279	42.0	0.0000090
6750	3.500	100.0	0.0000215	210.0	0.0000451	39.0	0.0000084
6750	3.625	100.0	0.0000215	275.0	0.0000590	78.0	0.0000167
6750	3.750	100.0	0.0000215	340.0	0.0000730	25.0	0.0000054
6750	3.875	100.0	0.0000215	340.0	0.0000730	36.5	0.0000078
6750	4.000	100.0	0.0000215	340.0	0.0000730	62.0	0.0000133
7000	1.000	100.0	0.0000200	81.0	0.0000162	12.5	0.0000025
7000	1.125	100.0	0.0000200	61.0	0.0000122	9.0	0.0000018
7000	1.250	100.0	0.0000200	78.0	0.0000156	9.5	0.0000019
7000	1.375	100.0	0.0000200	90.0	0.0000180	6.5	0.0000013
7000	1.500	100.0	0.0000200	120.0	0.0000240	7.5	0.0000015
7000	1.625	100.0	0.0000200	150.0	0.0000299	10.5	0.0000021
7000	1.750	100.0	0.0000200	145.0	0.0000289	9.5	0.0000019
7000	1.875	100.0	0.0000200	205.0	0.0000409	9.5	0.0000019
7000	2.000	100.0	0.0000200	340.0	0.0000679	12.5	0.0000025
7000	2.125	100.0	0.0000200	340.0	0.0000679	15.0	0.0000030
7000	2.250	100.0	0.0000200	300.0	0.0000599	13.5	0.0000027
7000	2.375	100.0	0.0000200	148.0	0.0000295	13.5	0.0000027
7000	2.500	100.0	0.0000200	180.0	0.0000359	13.5	0.0000027
7000	2.625	100.0	0.0000200	155.0	0.0000309	12.0	0.0000024
7000	2.750	100.0	0.0000200	150.0	0.0000299	12.0	0.0000024
7000	2.875	100.0	0.0000200	140.0	0.0000279	12.5	0.0000025
7000	3.000	100.0	0.0000200	125.0	0.0000249	11.0	0.0000022
7000	3.125	100.0	0.0000200	145.0	0.0000289	17.0	0.0000034
7000	3.250	100.0	0.0000200	160.0	0.0000319	12.5	0.0000025
7000	3.375	100.0	0.0000200	120.0	0.0000240	10.0	0.0000020
7000	3.500	100.0	0.0000200	130.0	0.0000259	7.5	0.0000015
7000	3.625	100.0	0.0000200	195.0	0.0000389	6.5	0.0000013
7000	3.750	100.0	0.0000200	340.0	0.0000679	12.0	0.0000024
7000	3.875	100.0	0.0000200	340.0	0.0000679	23.0	0.0000046
7000	4.000	100.0	0.0000200	290.0	0.0000579	11.0	0.0000022
7250	1.000	100.0	0.0000186	79.0	0.0000147	11.0	0.0000020
7250	1.125	100.0	0.0000186	41.0	0.0000076	9.5	0.0000018
7250	1.250	100.0	0.0000186	66.0	0.0000123	8.0	0.0000015
7250	1.375	100.0	0.0000186	62.0	0.0000115	6.5	0.0000012
7250	1.500	100.0	0.0000186	51.0	0.0000095	7.0	0.0000013
7250	1.625	100.0	0.0000186	50.0	0.0000093	8.5	0.0000016

Table 8. Load and Immersion of Probe Tip and Collet w.r.t. the Table (cont.)

Excitation Frequency (Hz)	Probe Immersion (inches)	Table Acceleration (Gs)	Table Displacement (inches)	Nylotron Collet Acceleration	Nylotron Collet Displacement	Probe Tip Acceleration (Gs)	Probe Tip Displacement (inches)
7250	1.750	100.0	0.0000186	77.0	0.0000143	8.5	0.0000016
7250	1.875	100.0	0.0000186	190.0	0.0000354	8.5	0.0000016
7250	2.000	100.0	0.0000186	340.0	0.0000633	11.0	0.0000020
7250	2.125	100.0	0.0000186	155.0	0.0000288	7.5	0.0000014
7250	2.250	100.0	0.0000186	98.0	0.0000182	9.5	0.0000018
7250	2.375	100.0	0.0000186	208.0	0.0000387	12.5	0.0000023
7250	2.500	100.0	0.0000186	108.0	0.0000201	10.0	0.0000019
7250	2.625	100.0	0.0000186	110.0	0.0000205	11.5	0.0000021
7250	2.750	100.0	0.0000186	120.0	0.0000223	13.5	0.0000025
7250	2.875	100.0	0.0000186	140.0	0.0000260	15.0	0.0000028
7250	3.000	100.0	0.0000186	110.0	0.0000205	13.0	0.0000024
7250	3.125	100.0	0.0000186	135.0	0.0000251	15.0	0.0000028
7250	3.250	100.0	0.0000186	175.0	0.0000326	15.5	0.0000029
7250	3.375	100.0	0.0000186	190.0	0.0000354	14.5	0.0000027
7250	3.500	100.0	0.0000186	330.0	0.0000614	14.0	0.0000026
7250	3.625	100.0	0.0000186	340.0	0.0000633	16.5	0.0000031
7250	3.750	100.0	0.0000186	340.0	0.0000633	25.0	0.0000047
7250	3.875	100.0	0.0000186	340.0	0.0000633	16.0	0.0000030
7250	4.000	100.0	0.0000186	195.0	0.0000363	12.0	0.0000022

Table 8. Load and Immersion of Probe Tip and Collet w.r.t. the Table (cont.)

Excitation Frequency (Hz)	Probe Immersion (inches)	Table Acceleration (Gs)	Table Displacement (inches)	Nylotron Collet Acceleration	Nylotron Collet Displacement	Probe Tip Acceleration (Gs)	Probe Tip Displacement (inches)
6000	1.000	118.0	0.0000321	100.0	0.0000272	28.0	0.0000076
6000	1.125	100.0	0.0000272	100.0	0.0000272	30.0	0.0000082
6000	1.250	110.0	0.0000299	100.0	0.0000272	33.0	0.0000090
6000	1.375	115.0	0.0000312	100.0	0.0000272	35.0	0.0000095
6000	1.500	120.0	0.0000326	100.0	0.0000272	35.5	0.0000096
6000	1.625	130.0	0.0000353	100.0	0.0000272	34.0	0.0000092
6000	1.750	71.0	0.0000193	100.0	0.0000272	25.0	0.0000068
6000	1.875	50.0	0.0000136	100.0	0.0000272	14.5	0.0000039
6000	2.000	42.0	0.0000114	100.0	0.0000272	9.0	0.0000024
6000	2.125	77.0	0.0000209	100.0	0.0000272	14.0	0.0000038
6000	2.250	12.0	0.0000033	100.0	0.0000272	3.0	0.0000008
6000	2.375	69.0	0.0000187	100.0	0.0000272	12.0	0.0000033
6000	2.500	48.0	0.0000130	100.0	0.0000272	9.5	0.0000026
6000	2.625	155.0	0.0000421	100.0	0.0000272	34.0	0.0000092
6000	2.750	120.0	0.0000326	100.0	0.0000272	20.5	0.0000056
6000	2.875	108.0	0.0000293	100.0	0.0000272	12.0	0.0000033
6000	3.000	100.0	0.0000272	100.0	0.0000272	14.5	0.0000039
6000	3.125	70.0	0.0000190	100.0	0.0000272	6.5	0.0000018
6000	3.250	40.0	0.0000109	100.0	0.0000272	3.5	0.0000010

Table 9. Load and Immersion of Probe Tip and Table w.r.t. the Collet (cont.)

Excitation Frequency (Hz)	Probe Immersion (inches)	Table Acceleration (Gs)	Table Displacement (inches)	Nylotron Collet Acceleration	Nylotron Collet Displacement	Probe Tip Acceleration (Gs)	Probe Tip Displacement (inches)
6000	3.375	25.0	0.0000068	100.0	0.0000272	6.5	0.0000018
6000	3.500	16.0	0.0000043	100.0	0.0000272	4.0	0.0000011
6000	3.625	14.0	0.0000038	100.0	0.0000272	3.5	0.0000010
6000	3.750	20.0	0.0000054	100.0	0.0000272	1.5	0.0000004
6000	3.875	19.0	0.0000052	100.0	0.0000272	1.5	0.0000004
6000	4.000	22.0	0.0000060	100.0	0.0000272	3.0	0.0000008
6250	1.000	100.0	0.0000250	100.0	0.0000250	29.0	0.0000073
6250	1.125	115.0	0.0000288	100.0	0.0000250	33.5	0.0000084
6250	1.250	130.0	0.0000325	100.0	0.0000250	31.0	0.0000078
6250	1.375	170.0	0.0000426	100.0	0.0000250	43.0	0.0000108
6250	1.500	175.0	0.0000438	100.0	0.0000250	43.0	0.0000108
6250	1.625	160.0	0.0000401	100.0	0.0000250	38.0	0.0000095
6250	1.750	160.0	0.0000401	100.0	0.0000250	34.5	0.0000086
6250	1.875	110.0	0.0000275	100.0	0.0000250	25.5	0.0000064
6250	2.000	71.0	0.0000178	100.0	0.0000250	13.0	0.0000033
6250	2.125	59.0	0.0000148	100.0	0.0000250	11.0	0.0000028
6250	2.250	31.0	0.0000078	100.0	0.0000250	5.0	0.0000013
6250	2.375	34.0	0.0000085	100.0	0.0000250	10.5	0.0000026
6250	2.500	44.0	0.0000110	100.0	0.0000250	16.5	0.0000041
6250	2.625	160.0	0.0000401	100.0	0.0000250	30.0	0.0000075
6250	2.750	54.0	0.0000135	100.0	0.0000250	25.5	0.0000064
6250	2.875	55.0	0.0000138	100.0	0.0000250	27.0	0.0000068
6250	3.000	76.0	0.0000190	100.0	0.0000250	33.0	0.0000083
6250	3.125	78.0	0.0000195	100.0	0.0000250	11.0	0.0000028
6250	3.250	100.0	0.0000250	100.0	0.0000250	48.0	0.0000120
6250	3.375	120.0	0.0000300	100.0	0.0000250	55.0	0.0000138
6250	3.500	125.0	0.0000313	100.0	0.0000250	63.0	0.0000158
6250	3.625	125.0	0.0000313	100.0	0.0000250	39.0	0.0000098
6250	3.750	90.0	0.0000225	100.0	0.0000250	16.0	0.0000040
6250	3.875	85.0	0.0000213	100.0	0.0000250	17.5	0.0000044
6250	4.000	68.0	0.0000170	100.0	0.0000250	11.5	0.0000029
6500	1.000	41.0	0.0000095	100.0	0.0000231	29.0	0.0000067
6500	1.125	69.0	0.0000160	100.0	0.0000231	24.0	0.0000056
6500	1.250	66.0	0.0000153	100.0	0.0000231	31.0	0.0000072
6500	1.375	66.0	0.0000153	100.0	0.0000231	30.5	0.0000071
6500	1.500	57.0	0.0000132	100.0	0.0000231	31.5	0.0000073
6500	1.625	160.0	0.0000370	100.0	0.0000231	38.0	0.0000088
6500	1.750	34.0	0.0000079	100.0	0.0000231	22.0	0.0000051
6500	1.875	26.0	0.0000060	100.0	0.0000231	15.0	0.0000035
6500	2.000	9.0	0.0000021	100.0	0.0000231	3.5	0.0000008
6500	2.125	8.0	0.0000019	100.0	0.0000231	3.5	0.0000008
6500	2.250	27.0	0.0000062	100.0	0.0000231	12.0	0.0000028
6500	2.375	68.0	0.0000157	100.0	0.0000231	47.0	0.0000109
6500	2.500	35.0	0.0000081	100.0	0.0000231	18.5	0.0000043
6500	2.625	46.0	0.0000106	100.0	0.0000231	29.0	0.0000067
6500	2.750	65.0	0.0000150	100.0	0.0000231	42.0	0.0000097
6500	2.875	110.0	0.0000255	100.0	0.0000231	90.0	0.0000208
6500	3.000	115.0	0.0000266	100.0	0.0000231	77.0	0.0000178
6500	3.125	80.0	0.0000185	100.0	0.0000231	55.0	0.0000127
6500	3.250	72.0	0.0000167	100.0	0.0000231	46.5	0.0000108

Table 9. Load and Immersion of Probe Tip and Table w.r.t. the Collet (cont.)

Excitation Frequency (Hz)	Probe Immersion (inches)	Table Acceleration (Gs)	Table Displacement (inches)	Nylotron Collet Acceleration	Nylotron Collet Displacement	Probe Tip Acceleration (Gs)	Probe Tip Displacement (inches)
6500	3.375	64.0	0.0000148	100.0	0.0000231	43.0	0.0000100
6500	3.500	58.0	0.0000134	100.0	0.0000231	34.5	0.0000080
6500	3.625	45.0	0.0000104	100.0	0.0000231	26.5	0.0000061
6500	3.750	33.0	0.0000076	100.0	0.0000231	16.0	0.0000037
6500	3.875	16.0	0.0000037	100.0	0.0000231	10.5	0.0000024
6500	4.000	10.0	0.0000023	100.0	0.0000231	4.0	0.0000009
6750	1.000	54.0	0.0000116	100.0	0.0000215	19.0	0.0000041
6750	1.125	39.0	0.0000084	100.0	0.0000215	13.0	0.0000028
6750	1.250	29.0	0.0000062	100.0	0.0000215	12.0	0.0000026
6750	1.375	33.0	0.0000071	100.0	0.0000215	13.5	0.0000029
6750	1.500	45.0	0.0000097	100.0	0.0000215	16.0	0.0000034
6750	1.625	47.0	0.0000101	100.0	0.0000215	14.5	0.0000031
6750	1.750	42.0	0.0000090	100.0	0.0000215	16.5	0.0000035
6750	1.875	32.0	0.0000069	100.0	0.0000215	8.0	0.0000017
6750	2.000	9.0	0.0000019	100.0	0.0000215	3.5	0.0000008
6750	2.125	3.5	0.0000008	100.0	0.0000215	5.5	0.0000012
6750	2.250	12.0	0.0000026	100.0	0.0000215	11.5	0.0000025
6750	2.375	7.0	0.0000015	100.0	0.0000215	6.5	0.0000014
6750	2.500	13.0	0.0000028	100.0	0.0000215	9.5	0.0000020
6750	2.625	16.0	0.0000034	100.0	0.0000215	12.0	0.0000026
6750	2.750	16.0	0.0000034	100.0	0.0000215	12.5	0.0000027
6750	2.875	22.0	0.0000047	100.0	0.0000215	15.0	0.0000032
6750	3.000	38.0	0.0000082	100.0	0.0000215	21.5	0.0000046
6750	3.125	110.0	0.0000236	100.0	0.0000215	50.0	0.0000107
6750	3.250	110.0	0.0000236	100.0	0.0000215	36.0	0.0000077
6750	3.375	73.0	0.0000157	100.0	0.0000215	28.0	0.0000060
6750	3.500	45.0	0.0000097	100.0	0.0000215	19.0	0.0000041
6750	3.625	34.0	0.0000073	100.0	0.0000215	13.0	0.0000028
6750	3.750	20.0	0.0000043	100.0	0.0000215	7.5	0.0000016
6750	3.875	8.5	0.0000018	100.0	0.0000215	2.5	0.0000005
6750	4.000	4.0	0.0000009	100.0	0.0000215	4.5	0.0000010
7000	1.000	120.0	0.0000240	100.0	0.0000200	16.0	0.0000032
7000	1.125	165.0	0.0000329	100.0	0.0000200	14.0	0.0000028
7000	1.250	135.0	0.0000269	100.0	0.0000200	13.0	0.0000026
7000	1.375	115.0	0.0000230	100.0	0.0000200	7.5	0.0000015
7000	1.500	80.0	0.0000160	100.0	0.0000200	6.0	0.0000012
7000	1.625	70.0	0.0000140	100.0	0.0000200	22.0	0.0000044
7000	1.750	71.0	0.0000142	100.0	0.0000200	6.5	0.0000013
7000	1.875	52.0	0.0000104	100.0	0.0000200	4.5	0.0000009
7000	2.000	27.0	0.0000054	100.0	0.0000200	3.0	0.0000006
7000	2.125	13.0	0.0000026	100.0	0.0000200	2.5	0.0000005
7000	2.250	31.0	0.0000062	100.0	0.0000200	4.5	0.0000009
7000	2.375	70.0	0.0000140	100.0	0.0000200	6.5	0.0000013
7000	2.500	56.0	0.0000112	100.0	0.0000200	8.0	0.0000016
7000	2.625	64.0	0.0000128	100.0	0.0000200	8.0	0.0000016
7000	2.750	67.0	0.0000134	100.0	0.0000200	8.0	0.0000016
7000	2.875	71.0	0.0000142	100.0	0.0000200	9.0	0.0000018
7000	3.000	80.0	0.0000160	100.0	0.0000200	9.0	0.0000018
7000	3.125	69.0	0.0000138	100.0	0.0000200	8.5	0.0000017
7000	3.250	62.0	0.0000124	100.0	0.0000200	8.0	0.0000016

Table 9. Load and Immersion of Probe Tip and Table w.r.t. the Collet (cont.)

Excitation Frequency (Hz)	Probe Immersion (inches)	Table Acceleration (Gs)	Table Displacement (inches)	Nylotron Collet Acceleration	Nylotron Collet Displacement	Probe Tip Acceleration (Gs)	Probe Tip Displacement (inches)
7000	3.375	82.0	0.0000164	100.0	0.0000200	8.0	0.0000016
7000	3.500	77.0	0.0000154	100.0	0.0000200	5.5	0.0000011
7000	3.625	55.0	0.0000110	100.0	0.0000200	3.0	0.0000006
7000	3.750	23.0	0.0000046	100.0	0.0000200	1.5	0.0000003
7000	3.875	8.0	0.0000016	100.0	0.0000200	3.0	0.0000006
7000	4.000	32.0	0.0000064	100.0	0.0000200	4.0	0.0000008
7250	1.000	130.0	0.0000242	100.0	0.0000186	15.0	0.0000028
7250	1.125	230.0	0.0000428	100.0	0.0000186	22.5	0.0000042
7250	1.250	140.0	0.0000260	100.0	0.0000186	14.0	0.0000026
7250	1.375	150.0	0.0000279	100.0	0.0000186	10.5	0.0000020
7250	1.500	230.0	0.0000428	100.0	0.0000186	16.0	0.0000030
7250	1.625	285.0	0.0000530	100.0	0.0000186	19.5	0.0000036
7250	1.750	140.0	0.0000260	100.0	0.0000186	12.0	0.0000022
7250	1.875	51.0	0.0000095	100.0	0.0000186	4.0	0.0000007
7250	2.000	25.0	0.0000047	100.0	0.0000186	3.0	0.0000006
7250	2.125	63.0	0.0000117	100.0	0.0000186	4.5	0.0000008
7250	2.250	105.0	0.0000195	100.0	0.0000186	10.0	0.0000019
7250	2.375	51.0	0.0000095	100.0	0.0000186	5.5	0.0000010
7250	2.500	94.0	0.0000175	100.0	0.0000186	9.0	0.0000017
7250	2.625	93.0	0.0000173	100.0	0.0000186	10.5	0.0000020
7250	2.750	71.0	0.0000132	100.0	0.0000186	9.5	0.0000018
7250	2.875	68.0	0.0000127	100.0	0.0000186	10.5	0.0000020
7250	3.000	90.0	0.0000167	100.0	0.0000186	11.5	0.0000021
7250	3.125	73.0	0.0000136	100.0	0.0000186	11.0	0.0000020
7250	3.250	55.0	0.0000102	100.0	0.0000186	8.5	0.0000016
7250	3.375	52.0	0.0000097	100.0	0.0000186	7.5	0.0000014
7250	3.500	34.0	0.0000063	100.0	0.0000186	4.5	0.0000008
7250	3.625	17.0	0.0000032	100.0	0.0000186	2.5	0.0000005
7250	3.750	13.0	0.0000024	100.0	0.0000186	1.5	0.0000003
7250	3.875	29.0	0.0000054	100.0	0.0000186	4.0	0.0000007
7250	4.000	52.0	0.0000097	100.0	0.0000186	6.0	0.0000011

Table 9. Load and Immersion of Probe Tip and Table w.r.t. the Collet (cont.)

All tolerances ± 0.005 unless
otherwise indicated

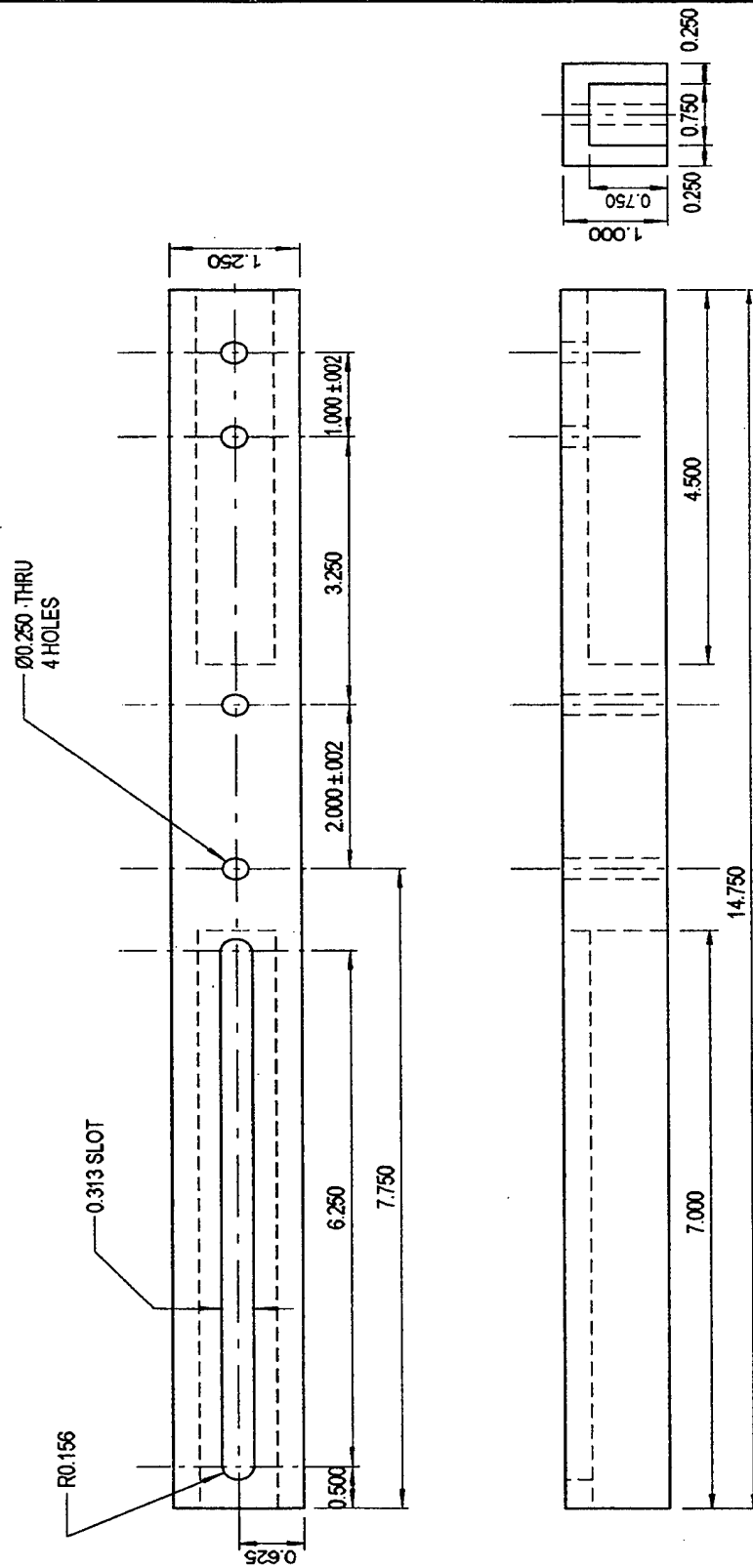
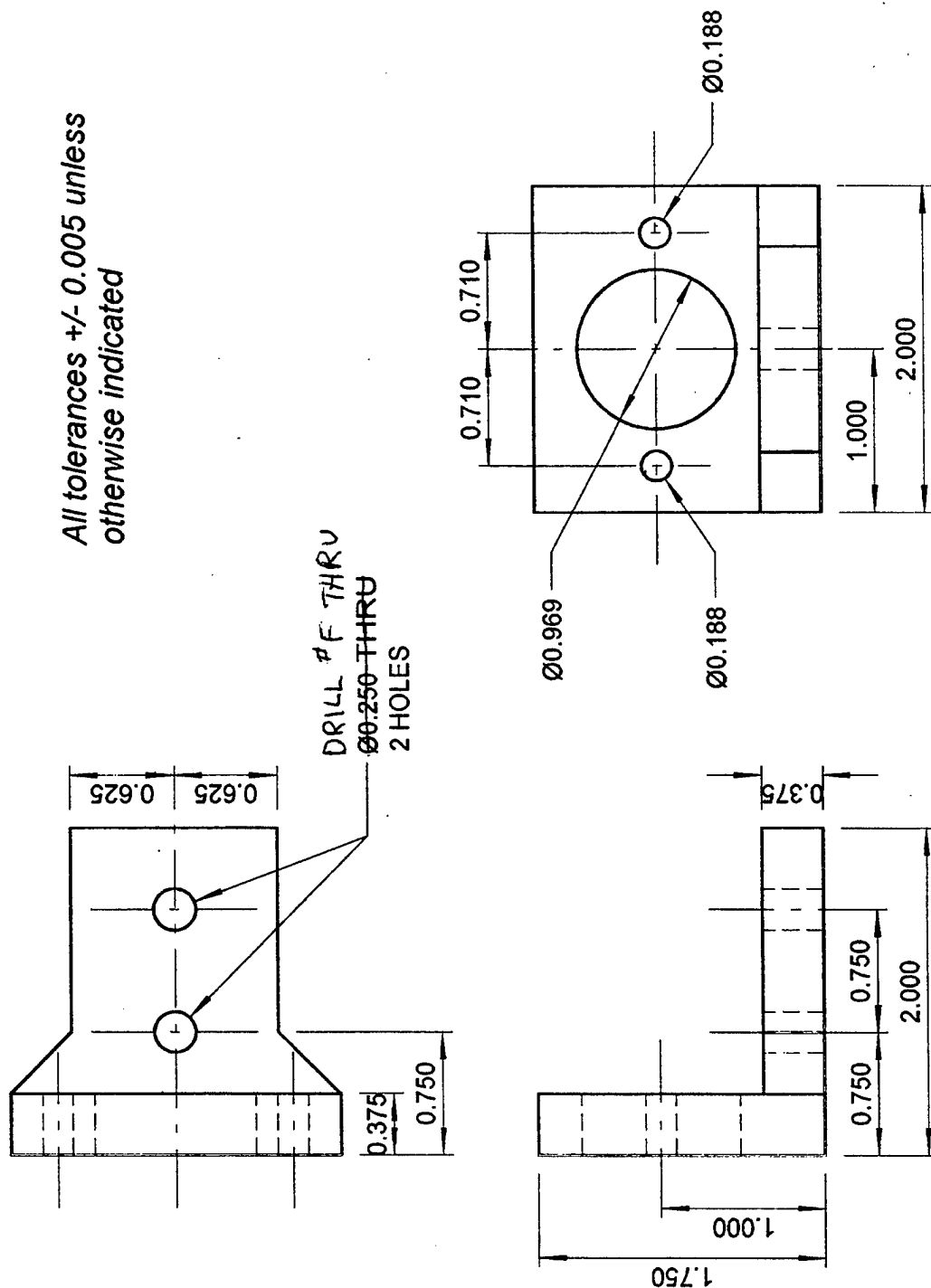


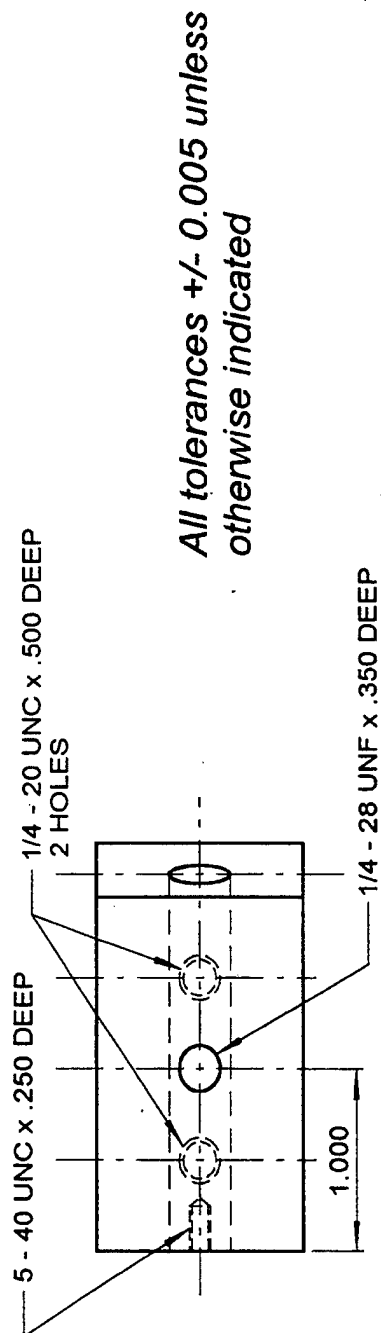
Figure 19. Schematic of Jig Base

Name: Jig Base	Scale: Inches
Mat.: Aluminum Alloy 5160	Date: 8/5/94
Dr: Lt. C Cunningham	POTF Ph: 64738



Name: Movable Mount	Scale: Full (in.)
Mat.: Aluminum Alloy 6061	Date: 8/5/94
Dr: Lt. C Cunningham POTF	Ph: 54738

Figure 20. Schematic of Movable Mount



All tolerances ± 0.005 unless otherwise indicated

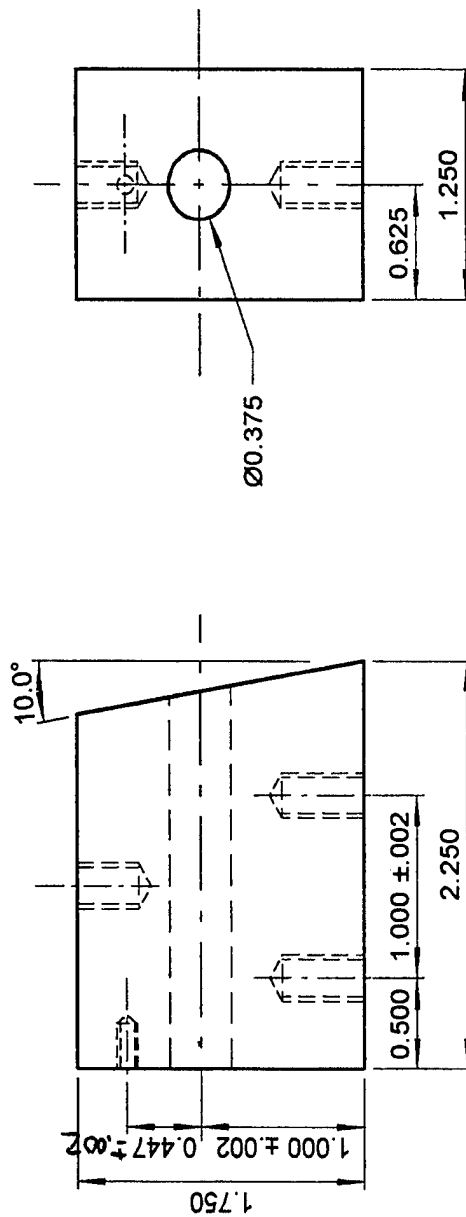


Figure 21. Schematic of Fixed Mount

Name: Fixed Mount	Scale: Full (in.)
Mat.: Aluminum Alloy 6061	Date: 8/5/94
Dr: Lt. C Cunningham	POTF Ph: 54738

REFERENCES

1. Beer, F. P., and Johnston, E. R., Vector Mechanics for Engineers : Statics, 5th Edition, McGraw-Hill, New York NY, 1988
2. Gere, J. M., and Timoshenko, S. P., Mechanics of Materials, 2nd Edition, PWS-Kent Publishing Company, Boston MA, 1984
3. Janna, William S., Introduction to Fluid Mechanics, Wadsworth Inc., Belmont CA, 1983.
4. Harris, Cyril M. and Crede, Charles E. (editors), Shock & Vibration Handbook, McGraw-Hill, Inc., 1976.
5. Vierck, Robert K., Vibrational Analysis, Arper & Row, Publishers, New York NY, 1979.
6. "Experiments in Structural Dynamics: Natural Frequency of Cantilever Beams", Dept. of Aeronautical and Astronautical Engineering, The Ohio State University.